

Rhodium(I) and Iridium(I) Complexes with β -Keto Phosphine or Phosphino Enolate Ligands. Catalytic Transfer Dehydrogenation of Cyclooctane[†]

Pierre Braunstein,^{*,‡} Yves Chauvin,^{*,§} Jens Nähring,^{‡,§} André DeCian,^{||}
Jean Fischer,^{||} Antonio Tiripicchio,[⊥] and Franco Ugozzoli[⊥]

Laboratoire de Chimie de Coordination, Associé au CNRS (URA 416), Université Louis Pasteur, 4 rue Blaise Pascal, F-67070 Strasbourg Cédex, France, Institut Français du Pétrole, B.P. 311, F-92506 Reuil-Malmaison Cédex, France, Laboratoire de Cristallographie et de Chimie Structurale, Associé au CNRS (URA 424), Université Louis Pasteur, 4 rue Blaise Pascal, F-67070 Strasbourg Cédex, France, and Dipartimento di Chimica Generale ed Inorganica, Chimica Analitica, Chimica Fisica, Università di Parma, Centro di Studio per la Strutturistica Diffattometrica del CNR, Viale delle Scienze 78, I-43100 Parma, Italy

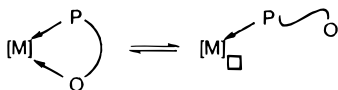
Received June 21, 1996[Ⓢ]

The synthesis of new metal complexes containing the keto phosphine ligands $R^1_2PCH_2C(O)R^2$ ($R^1 = Ph$, $R^2 = Ph$, Me , $t-Bu$, $p-C_6H_4F$; $R^1 = i-Pr$, $R^2 = Ph$) is described. Reaction of 1 equiv of (diphenylphosphino)acetophenone ($Ph_2PCH_2C(O)Ph$; **L**) with $[Rh(\mu-Cl)(C_2H_4)_2]_2$ gave the dimeric complex $[Rh(\mu-Cl)(C_2H_4)(P\sim O)]_2$ (**1**) ($P\sim O = \eta^1(P)$ coordinated). With 2 equiv of **L**, $[RhCl(P\sim O)(P\sim O)]$ (**2**) was obtained ($P\sim O = \eta^2(P, O)$ -chelated ligand). Reaction of **2** with $TiPF_6$ afforded the cationic complex $[Rh(P\sim O)_2][PF_6]$ (**3**). The X-ray crystal structure determination of **3**·H₂O shows a distorted-square-planar geometry with the two phosphorus atoms (and oxygen atoms) in *cis* positions. Treatment of $[RhCl(CO)(PPh_3)_2]$ with 1 equiv of **L** gave $[RhCl(CO)(P\sim O)(PPh_3)]$ (**5**). In the presence of $TiPF_6$ the cationic complex $[Rh(CO)(P\sim O)(PPh_3)][PF_6]$ (**6**) was obtained. The X-ray crystal structure determination of **6** shows a slightly distorted square planar geometry with the two phosphorus atoms in *trans* positions. The reaction of **5** or **6** with 1 equiv of NaOMe produced the phosphino enolate complex $[Rh\{Ph_2PCH_2C(\sim O)Ph\}(CO)(PPh_3)]$ (**7**). ³¹P{¹H} NMR shows **7** to dissociate PPh₃ in solution, giving a 14-electron species, which proved to be particularly useful for transfer-dehydrogenation reactions. When $[Rh(\mu-Cl)(COE)_2]_2$ (COE = cyclooctene) was reacted with 4 equiv of **L** under carbon monoxide, $[RhCl(CO)(P\sim O)_2]$ (**8**) was isolated. Reaction of **8** with $TiPF_6$ gave $[Rh(CO)(P\sim O)(P\sim O)][PF_6]$ (**9**), and in the presence of NaOMe the phosphino enolate complex $[Rh\{Ph_2PCH_2C(\sim O)Ph\}(CO)(P\sim O)]$ (**10**) formed. In an analogous manner, $[Rh\{Ph_2PCH_2C(\sim O)Ph\}(CO)L^1]$ ($L^1 = P(o\text{-tolyl})_3$ (**11**), $PPh_2(p\text{-tolyl})$ (**12**), $P(p\text{-C}_6\text{H}_4\text{F})_3$ (**13**)) were also prepared. In a similar way, **L** and $[RhCl(PPh_3)_3]$ gave $[RhCl(PPh_3)_2(P\sim O)]$ (**14**), which was reacted with $TiPF_6$, affording $[Rh(P\sim O)(PPh_3)_2][PF_6]$ (**15**), analogous to **6**. Reacting **14** or **15** with 1 equiv of NaOMe gave the phosphino enolate complex $[Rh\{Ph_2PCH_2C(\sim O)Ph\}(PPh_3)_2]$ (**16**), analogous to **7**. It reacts with PhNCO or Ph₂PCl with formation of a C_{enolate}–C or O_{enolate}–P bond, respectively. $[Rh\{Ph_2PCH_2C(\sim O)Ph\}(p\text{-C}_6\text{H}_4\text{F})\}(PPh_3)_2]$ (**17**) has also been reported. By reacting PPh₃, **L**, and $TiPF_6$ with $[Rh(\mu-Cl)(NBD)]_2$ (NBD = norbornadiene) the pentacoordinated complex $[Rh(NBD)(P\sim O)(PPh_3)][PF_6]$ (**20**) was obtained. The X-ray crystal structure determination of **20** showed that the coordination geometry around the Rh atom could be described as intermediate between square pyramidal (with the O atom occupying the apical position) and trigonal bipyramidal (with the P atom and the midpoint of one olefinic bond occupying the apical positions). When the diolefin, **L**, and NaOMe were added in sequence to a suspension of $[Rh(\mu-Cl)(COE)_2]_2$, $[Rh\{Ph_2PCH_2C(\sim O)Ph\}(NBD)]$ (**21**) and $[Rh\{Ph_2PCH_2C(\sim O)Ph\}(COD)]$ (**22**) were obtained. The related iridium complex $[Ir\{Ph_2PCH_2C(\sim O)Ph\}(COD)]$ (**26**) was obtained in a similar way and reacted with H₂ to give $[Ir\{Ph_2PCH_2C(\sim O)Ph\}H_2(COD)]$ (**27**). The cationic complex **20** and the phosphino enolate complexes **4**, **7**, and **16** catalyze the hydrogenation and the isomerization of 1-hexene. The rhodium phosphino enolate carbonyl complexes **7** and **13** are very active catalysts for transfer dehydrogenation of cyclooctane with norbornene under hydrogen pressure (7 MPa) at 60–90 °C. In the presence of 1 equiv of a triarylphosphine, rhodium phosphino enolate complexes not containing carbon monoxide, such as **22**, proved to be active catalysts for transfer dehydrogenation at 70 °C, under atmospheric pressure of hydrogen, with turnover numbers up to 240 per mol of rhodium/h.

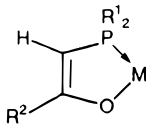
Introduction

Homogeneous catalysis by transition-metal complexes plays an important role in industrial chemistry.² Neutral and cationic complexes of rhodium(I) are versatile catalysts for hydrogenation, isomerization, dimerization, hydroformylation, and carbonylation reactions.³ Most of these complexes are stabilized by tertiary phosphines. In the catalytic steps, solvent molecules play a crucial role and ketones, alcohols, or ethers, weakly bonded to the coordinatively unsaturated rhodium center, help stabilize reactive intermediates.⁴

In complexes containing phosphorus and oxygen (or nitrogen) heterobidentate ligands, the "hard" donor moiety can be considered as an intramolecular solvent molecule, which may dissociate from the metal reversibly. This allows the use of a noncoordinating solvent in catalytic reactions. The hemilability of ether, ester, and keto phosphine ligands is well-documented.⁵



It is also known that phosphino enolate ligands of the type $[R^1_2PCH=C(O)R^2]^-$ can be readily obtained from the corresponding β -keto phosphines. They behave as three-electron donors ($2(P) + 1(O)$) and stabilize the square-planar structure of several transition-metal complexes.⁶



These important features have led to the development of very active and selective catalysts for various reactions. Thus, a palladium(II) complex containing 2-(diphenylphosphino)pyridine as a hemilabile heterobidentate ligand catalyzes the carbonylation of propyne to methyl methacrylate with very high efficiency.⁷ Three-electron-donor enolate-type chelates confer to their nickel(II) complexes unique catalytic properties for the formation of α -olefins from ethylene.⁸

Recently the catalytic transfer dehydrogenation of alkanes using rhodium(I) complexes was reported in the

literature.⁹ The reaction mechanism probably involves square-planar/octahedral interconversions of the metal coordination sphere. This led us to investigate the coordination modes of β -keto phosphines and related phosphino enolates to rhodium(I) in relation to the catalytic activity of the corresponding complexes in hydrogenation of olefins and transfer dehydrogenation of alkanes.

Results and Discussion

1. Preparation of β -Keto Phosphines. In order to prepare β -keto phosphines of the type $R^1_2PCH_2C(O)R^2$ Lutsenko *et al.* reacted chlorophosphines with mercury or stannyl ketones,¹⁰ while Shaw *et al.* reacted di-*tert*-butylphosphine with bromomethyl ketones, followed by treatment with a base.¹¹ The latter method fails for $R^2 = Me$.¹² Other methods involve the reduction of a functional phosphine oxide with a silane under reflux or the simultaneous reduction and complexation of a functional phosphine sulfide on nickel(II) followed by decomplexation.¹³ Whereas the reaction of chloromethyl ketones with sodium diphenylphosphide did not yield β -keto phosphines,¹⁴ and that of lithium diphenylphosphide with (1*R*)-*endo*-(+)-3-bromocamphor in THF at $-78^\circ C$ led only to tetraphenyldiphosphine,¹⁵ we have found that the reaction of $LiPPh_2$ and chloroacetone under similar conditions yielded a mixture of diphenylphosphine (60%) and the β -keto phosphine $Ph_2PCH_2C(O)Me$ (38%); the latter was isolated by distillation in 25% yield.

(Diphenylphosphino)acetophenone, $Ph_2PCH_2C(O)Ph$ (**L**), is readily synthesized by the reaction of the lithium enolate of acetophenone with diphenylchlorophosphine at $-78^\circ C$ in THF.⁶ This method was easily extended to other chlorophosphines and ketones (see Experimental Section). Under these reaction conditions, no O–P coupling occurred, probably because in THF the lithium cation is closely associated with the oxygen atom of the enolate, which directs the reactivity of the ambident anion to the carbon atom.¹⁶ Our method has since been successfully applied to the synthesis of various diphenylphosphino ketones.¹⁷

(8) (a) Keim, W. *Chem.-Ing.-Techn.* **1984**, 56, 850. (b) Klabunde, U.; Tulip, T. H.; Roe, D. C.; Ittel, S. D. *J. Organomet. Chem.* **1987**, 334, 141. (c) Keim, W. *Angew. Chem., Int. Ed. Engl.* **1990**, 29, 235. (d) Mercier, S. Ph.D. Thesis, Université Paris VI, 1993. (e) Keim, W. *New J. Chem.* **1994**, 18, 93. (f) Braunstein, P.; Chauvin, Y.; Mercier, S.; Saussine, L.; DeCian, A.; Fischer, J. *J. Chem. Soc., Chem. Commun.* **1994**, 2203.

(9) (a) Maguire, J. A.; Goldman, A. S. *J. Am. Chem. Soc.* **1991**, 113, 6706. (b) Maguire, J. A.; Petrillo, A.; Goldman, A. S. *J. Am. Chem. Soc.* **1992**, 114, 9492. (c) Shih, K.-C.; Goldman, A. S. *Organometallics* **1993**, 12, 3390. (d) Miller, J. A.; Knox, L. K. *J. Chem. Soc., Chem. Commun.* **1994**, 1449.

(10) (a) Novikova, Z. S.; Proskurnina, M. V.; Petrovskaya, L. I.; Bogdanova, I. V.; Galitskova, N. P.; Lutsenko, I. F. *J. Gen. Chem. USSR (Engl. Transl.)* **1967**, 37, 1972. (b) Novikova, Z. S.; Galitskova, N. P.; Kozlov, V. A.; Lutsenko, I. F. *J. Gen. Chem. USSR (Engl. Transl.)* **1971**, 41, 838.

(11) Moulton, C. J.; Shaw, B. L. *J. Chem. Soc., Dalton Trans.* **1980**, 299.

(12) (a) Brunner, H.; Dylla, M. E.; Hecht, G. A. M.; Pieronczyk, W. *Z. Naturforsch.* **1982**, 37B, 404. (b) Dylla, M. E. Zulassungsarbeit, Universität Regensburg, 1980.

(13) Braunstein, P.; Matt, D.; Mathey, F.; Thavard, D. *J. Chem. Res., Miniprint* **1978**, 3041; *J. Chem. Res., Synop.* **1978**, 232.

(14) Eibach, F. Diplomarbeit, Universität Marburg, 1976.

(15) Knight, D. A.; Cole-Hamilton, D. J.; Cupertino, D. C. *J. Chem. Soc., Dalton Trans.* **1990**, 3051.

(16) Streitweiser, A.; Heathcock, C. H. In *Einführung in die organische Chemie*; Macmillan: New York, 1980; p 483.

(17) Demerseman, B.; Guilbert, B.; Renouard, C.; Gonzalez, M.; Dixneuf, P. H. *Organometallics* **1993**, 12, 3906.

[†] Dedicated to Professor G.E. Herberich, on the occasion of his 60th birthday, with our sincere congratulations and best wishes. Part of the Doctoral Thesis of J.N. Complexes with Functional Phosphines. For previous parts in this series, see ref 1.

[‡] Laboratoire de Chimie de Coordination, Université Louis Pasteur.

[§] Institut Français du Pétrole.

[¶] Laboratoire de Cristallographie et de Chimie Structurale, Université Louis Pasteur.

[‡] Università di Parma.

^{*} Abstract published in *Advance ACS Abstracts*, November 1, 1996. (1) (a) Braunstein, P.; Chauvin, Y.; Nähring, J.; DeCian, A.; Fischer, J. *J. Chem. Soc., Dalton Trans.* **1995**, 863. (b) Braunstein, P.; Chauvin, Y.; Nähring, J.; Dusauroy, Y.; Tiripicchio, A.; Ugozzoli, F. *J. Chem. Soc., Dalton Trans.* **1995**, 851.

(2) Parshall, G. W.; Ittel, S. D. *Homogeneous Catalysis*, 2nd ed.; Wiley: New York, 1992.

(3) Spencer, A. In *Comprehensive Coordination Chemistry*; Wilkinson, G.; Gillard, R. D.; McCleverty, J., Eds.; Pergamon Press: Oxford, England, 1987; Vol. 6, p. 229.

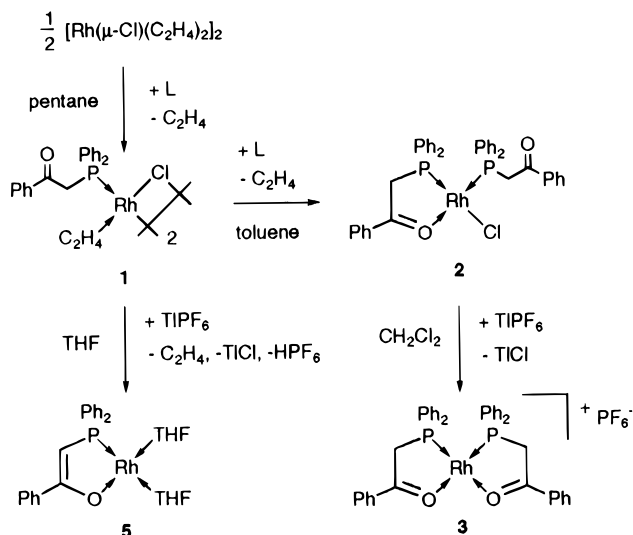
(4) Halpern, J. *Inorg. Chim. Acta* **1981**, 50, 11.

(5) Bader, A.; Lindner, E. *Coord. Chem. Rev.* **1991**, 108, 27.

(6) Bouaoud, S.-E.; Braunstein, P.; Grandjean, D.; Matt, D.; Nobel, D. *Inorg. Chem.* **1986**, 25, 3765.

(7) Drent, E.; Arnoldy, P.; Budzelaar, P. H. M. *J. Organomet. Chem.* **1993**, 455, 247.

Scheme 1



2. Rhodium(I) Complexes with $\text{Ph}_2\text{PCH}_2\text{C}(\text{O})\text{Ph}$. Reaction with $[\text{Rh}(\mu\text{-Cl})(\text{C}_2\text{H}_4)_2]_2$. Addition of 1 equiv of keto phosphine to a suspension of $[\text{Rh}(\mu\text{-Cl})(\text{C}_2\text{H}_4)_2]_2$ in pentane afforded the dimeric complex $[\text{Rh}(\mu\text{-Cl})(\text{C}_2\text{H}_4)(\text{P}(\text{Ph})_2\text{C}(\text{O})\text{Ph})]_2$ (**1**) (Scheme 1). The IR spectrum shows absorption bands at 272 and 258 cm^{-1} for the bridging chlorides and at 1523 cm^{-1} for ethylene. A band at 1665 cm^{-1} is attributed to the uncoordinated keto function. The $^{31}\text{P}\{^1\text{H}\}$ NMR spectrum shows a doublet with a $^1J(\text{RhP})$ value of 189 Hz, in keeping with a phosphine coordinated to a rhodium(I) center in a *trans* position with respect to a bridging chloride. A variable-temperature ^1H NMR study revealed rotation of ethylene around the bond axis. Even at 180 K rotation was not completely frozen, and its activation energy can be roughly estimated from the Eyring equation as inferior to 55 kJ mol^{-1} .¹⁸ This value is in the range found for $[\text{Rh}(\text{Cp})\text{L}^2(\text{C}_2\text{H}_4)]$ ($\text{L}^2 = \text{C}_2\text{H}_4, \text{C}_2\text{F}_4, \text{SO}_2$) complexes, with 62.6 ± 0.8 , 57 ± 3 , and 51 ± 3 kJ mol^{-1} , respectively.¹⁹

Complex **1** is stable toward ethylene elimination or splitting of the chloride bridges by the oxygen donor function of the potentially chelating keto phosphine. This is consistent with a keto oxygen being a weaker ligand than ethylene or a chloride in neutral rhodium(I) complexes, as no complex such as $[\text{Rh}(\mu\text{-Cl})(\text{P}(\text{Ph})_2\text{C}(\text{O})\text{Ph})]_2$ or $[\text{RhCl}(\text{olefin})(\text{P}(\text{Ph})_2\text{C}(\text{O})\text{Ph})]$ was formed.

Addition of 1 equiv of PPh_3 to a toluene or THF solution of **1** afforded a mixture of complexes, as shown by $^{31}\text{P}\{^1\text{H}\}$ NMR spectroscopy, but all PPh_3 was coordinated to rhodium. A strong band at 1670 cm^{-1} was characteristic of an uncoordinated keto group. These observations indicate that olefin substitution and bridge cleavage by PPh_3 in **1** need about the same energy and/or that the product redistributes its ligands. Addition of a second equivalent of PPh_3 afforded the unstable $[\text{RhCl}(\text{PPh}_3)_2(\text{P}(\text{Ph})_2\text{C}(\text{O})\text{Ph})]$ (**14**) (*vide infra*). For comparison, no mixed-phosphine complex of the type $[\text{PdCl}_2(\text{PR}_3)(\text{P}(\text{Ph})_2\text{C}(\text{O})\text{Ph})]$ has been isolated from a dinuclear palladium

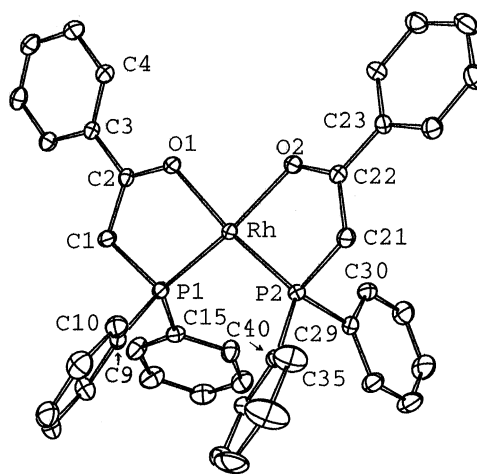


Figure 1. ORTEP plot of the cationic complex in $3 \cdot \text{H}_2\text{O}$, showing the numbering scheme used. Ellipsoids are scaled to enclose 50% of the electron density. Hydrogen atoms are omitted.

precursor,²⁰ although this has recently been achieved from palladium alkyl complexes.²¹ When **1** was reacted with 1 equiv of keto phosphine, ethylene was evolved and the bridge was split, affording the mononuclear compound $[\text{RhCl}(\text{P}(\text{Ph})_2\text{C}(\text{O})\text{Ph})_2]$ (**2**) (Scheme 1). It is thermally stable but decomposes in CH_2Cl_2 over weeks. IR spectroscopy indicates free and coordinated keto groups, and $^{31}\text{P}\{^1\text{H}\}$ NMR spectroscopy shows two mutually *cis* phosphines. Complex **2** is not fluxional at room temperature. Complexes of this type with ether-phosphine ligands have been recently reported by Lindner *et al.* and Werner *et al.*²² Their reactivity was found to depend on the substituents at phosphorus: with $\text{R} = \text{Ph}$ or Me , they were not fluxional in solution and were inert to hydrogen, whereas with $\text{R} = \text{cyclohexyl}$, fluxional behavior was observed and under a hydrogen atmosphere the unstable dihydridorhodium(III) complex $[\text{RhCl}(\text{H})_2\{\text{C}_2\text{P}(\text{CH}_2)_2\text{OMe}\}_2]$ was formed.

Reaction of **2** with an excess of TIPF_6 afforded air-stable red crystals of the square-planar cationic complex *cis*- $[\text{Rh}(\text{P}(\text{Ph})_2\text{C}(\text{O})\text{Ph})_2][\text{PF}_6]$ (**3**). The structure of the cation, determined by X-ray diffraction (Figure 1), is in agreement with the solution structure derived from other spectroscopic data: the two phosphorus atoms are in *cis* positions (for values of the chemical shift and Rh-P coupling constant, see the Experimental Section). The thermal stability of this cationic bis(chelate) complex is in marked contrast to that of the corresponding ether-phosphine complexes with $\text{R}_2\text{PCH}_2\text{CHOCH}_2\text{-CH}_2\text{CH}_2$ ($\text{R} = \text{Ph}, \text{Cy}, \text{C}_2\text{PCH}_2\text{CH}_2\text{OCH}_3$), which are unstable above -30°C even in the solid state.^{5,23}

(20) Braunstein, P.; Matt, D.; Nobel, D.; Balegroune, F.; Bouaoud, S.-E.; Grandjean, D.; Fischer, J. *J. Chem. Soc., Dalton Trans.* **1988**, 27, 353.

(21) Andrieu, J.; Braunstein, P.; Naud, F. *J. Chem. Soc., Dalton Trans.* **1996**, 2903.

(22) (a) Lindner, E.; Wang, Q.; Mayer, H. A.; Bader, A.; Kühbauch, H.; Wegner, P. *Organometallics* **1993**, *12*, 3291. (b) Lindner, E.; Wang, Q.; Mayer, H. A.; Bader, A. *J. Organomet. Chem.* **1993**, *458*, 229. (c) Werner, H.; Hampp, A.; Peters, K.; Peters, E. M.; Walz, L.; von Schnering, H. G. *Z. Naturforsch.* **1990**, *45B*, 1548. (d) Werner, H.; Hampp, A.; Windmüller, B. *J. Organomet. Chem.* **1992**, *435*, 169.

(23) Lindner, E.; Wang, Q.; Mayer, H. A.; Fawzi, R.; Steinmann, M. *Organometallics* **1993**, *12*, 1865.

(18) Günther, H. *NMR Spectroscopie*, 3rd ed.; Thieme Verlag: Stuttgart, Germany, 1992; p 310.

(19) Cramer, R.; Kline, J. B.; Roberts, J. D. *J. Am. Chem. Soc.* **1969**, *91*, 2519.

Recently the stable *cis*-phosphine-*cis*-ether complex $[\text{Rh}(\eta^4\text{-}\{\eta^5\text{-C}_5\text{H}_4\text{OCH}_2\text{CH}_2\text{PPh}_2\}_2\text{Fe})]\text{BF}_4$ has been reported.²⁴

In CH_2Cl_2 , **3** was slowly oxidized to the rhodium(III) complex *trans,cis,cis*- $[\text{RhCl}_2(\text{P}^{\sim}\text{O})_2][\text{PF}_6]$, which was identified by its ^1H NMR spectrum.^{1b} Under a hydrogen atmosphere, **3** does not form a hydride complex (^1H NMR). For similar complexes with ether-phosphines, the reactivity toward hydrogen depends on the basicity of the phosphorus donor: cyclohexyl or isopropyl substituents lead to hydride complexes, although unstable, whereas a phenyl group does not.^{22b,23,25}

Reaction of complex **3** with 1 or 2 equiv of NaOMe in toluene or an excess of NaH in THF generated the phosphino enolate ligand, but no pure product could be isolated. This transformation was evidenced by the replacement of the IR absorption at 1565 cm^{-1} of **3** by a new one around 1520 cm^{-1} .

Addition of TIPF_6 to a THF solution of **1** resulted in a slow color change, from red to almost black-red. Surprisingly, the IR spectrum showed no band in the usual range for an uncoordinated keto function but a strong band at 1520 cm^{-1} , which is characteristic for a phosphino enolate ligand. Accordingly, the ^1H NMR spectrum in C_6D_6 showed a doublet at δ 5.22 due to $^2J(\text{PH})$ coupling instead of the doublet found at δ 4.04 for **1**. This downfield value is characteristic of a phosphino enolate ligand. The presence of coordinated THF was inferred from ^1H NMR data. The $^{31}\text{P}\{^1\text{H}\}$ NMR spectrum contained a doublet at 47.6 ppm with $J(\text{RhP}) = 184\text{ Hz}$, consistent with the phosphorus atom being in a chelate and in a *trans* position with respect to an oxygen donor atom. These data are consistent with the solvento complex $[\text{Rh}\{\text{Ph}_2\text{PCH}=\text{C}(\text{O})\text{Ph}\}(\text{THF})_2]$ (**4**), although it could only be characterized spectroscopically in solution owing to its lability. The formation of an enolate complex without addition of a strong base is notable and illustrates the stability provided by the phosphino enolate chelating ligand in a square-planar geometry. Related deprotonation reactions have been observed in the synthesis of $[\text{RhCl}\{\text{Ph}_2\text{PCH}=\text{C}(\text{O})\text{Ph}\}(\text{P}^{\sim}\text{O})(\text{P}^{\sim}\text{O})][\text{PF}_6]$ ^{1a} and on addition of *t*-Bu₂PCH₂C(O)-*t*-Bu to an ethanolic solution of nickel-

(II) chloride with formation of *trans*- $[\text{Ni}\{\text{Bu}^t_2\text{PCH}=\text{C}(\text{O})\text{Bu}\}]$.¹¹ The presence in the IR spectrum of the reaction mixture of a weaker band at 1570 cm^{-1} is consistent with the cationic intermediate $[\text{Rh}(\text{P}^{\sim}\text{O})(\text{THF})_2][\text{PF}_6]$. Its formation would be related to the synthesis of $[(\eta^3\text{-C}_3\text{H}_5)\text{Pd}(\text{solvent})_2][\text{BF}_4]$ by addition of 2 equiv of AgBF_4 to MeNO₂ or MeCN solutions of $[(\eta^3\text{-C}_3\text{H}_5)\text{Pd}(\mu\text{-Cl})_2]$.²⁶

Reaction with *trans*- $[\text{RhCl}(\text{CO})(\text{PPh}_3)_2]$. Treatment of *trans*- $[\text{RhCl}(\text{CO})(\text{PPh}_3)_2]$ with 1 equiv of **L** in toluene afforded $[\text{RhCl}(\text{CO})(\text{P}^{\sim}\text{O})(\text{PPh}_3)]$ (**5**) (Scheme 2). When this reaction was performed in $\text{CH}_2\text{Cl}_2/\text{acetone}$ in the presence of 1 equiv of TIPF_6 , the orange cationic chelate complex $[\text{Rh}(\text{CO})(\text{P}^{\sim}\text{O})(\text{PPh}_3)][\text{PF}_6]$ (**6**) was isolated in high yield. In both complexes the two phos-

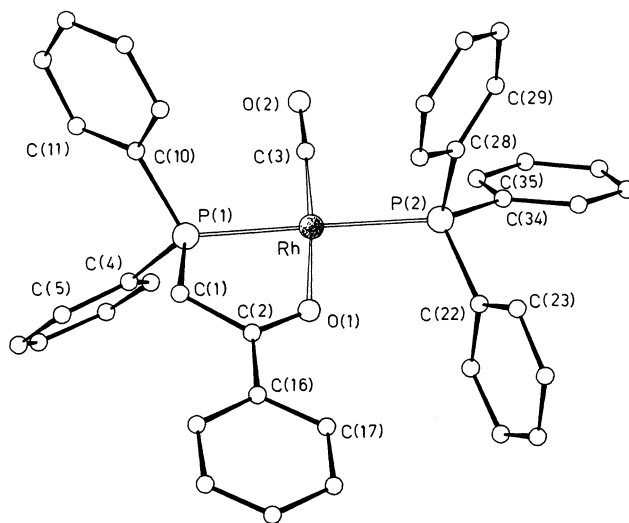
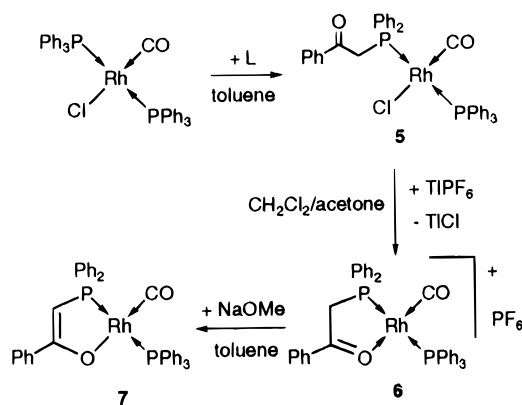


Figure 2. View of the structure of the cationic complex $[\text{Rh}(\text{CO})(\text{P}^{\sim}\text{O})(\text{PPh}_3)]^+$ in **6** with the atom-numbering scheme.

Scheme 2



phorus atoms are *trans* to each other ($^{31}\text{P}\{^1\text{H}\}$ NMR spectroscopy). The $\nu(\text{C}=\text{O})$ frequency for **6** was found at higher wavenumbers (1995 cm^{-1}) than for **5** (1974 cm^{-1}), in keeping with less electron density on rhodium being available in the former for back-bonding to $\text{C}=\text{O}$. The crystal structure of **6** (Figure 2) is in agreement with the structure in solution derived from spectroscopic data. The phosphino enolate complex $[\text{Rh}\{\text{Ph}_2\text{PCH}=\text{C}(\text{O})\text{Ph}\}(\text{CO})(\text{PPh}_3)]$ (**7**), which proved to be especially useful for alkane activation (see below), was obtained by reacting a toluene solution of **5** or a toluene suspension of **6** with 1 equiv of sodium methoxide in methanol. **7** could also be obtained by displacement of the acac ligand from $[\text{Rh}(\text{acac})(\text{PPh}_3)(\text{CO})]$ with the keto phosphine. Analytical and spectroscopic data support its formulation. The absorption of the $\text{C}=\text{O}$ stretching vibration was shifted to 1956 cm^{-1} , owing to the anionic oxygen donor, which confers more electron density to the metal. The absorption band at 1513 cm^{-1} is characteristic for the enolate ligand. The enolate proton gives in the ^1H NMR spectrum an overlapping doublet of doublets at 5.31 ppm with coupling constants $^2J(\text{PH})$ and $^3J(\text{RhH})$ of 2.2 Hz. The $^{31}\text{P}\{^1\text{H}\}$ spectrum at 200 K is typical for an ABX spin system (A = B = P, X = Rh), and the $^2J(\text{PP})$ coupling of 301 Hz for these two

(24) Allgeier, A. M.; Singewald, E. T.; Mirkin, C. A.; Stern, C. L. *Organometallics* **1994**, *13*, 2928.

(25) Lindner, E.; Wang, Q.; Mayer, H. A.; Fawzi, R.; Steinmann, M. *J. Organomet. Chem.* **1993**, *453*, 289.

(26) Sen, A.; Lai, T.-W. *Organometallics* **1983**, *2*, 1059.

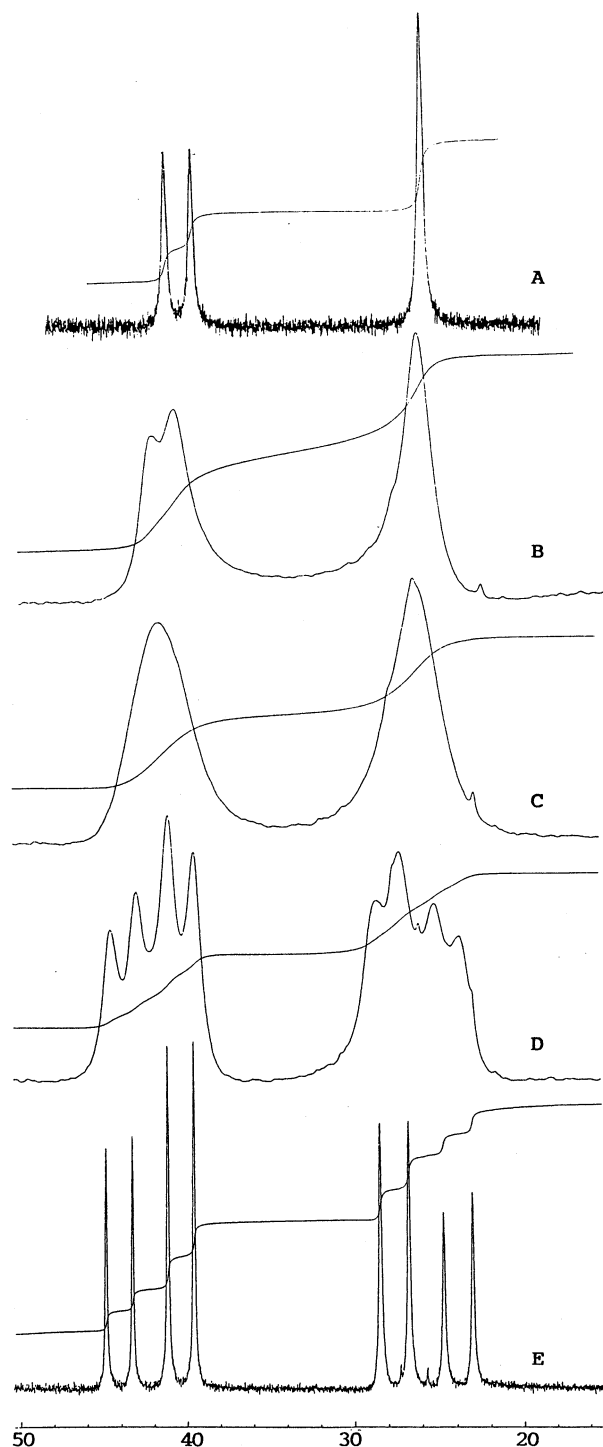
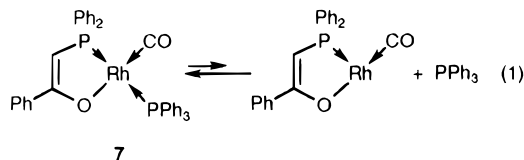


Figure 3. $^{31}\text{P}\{^1\text{H}\}$ NMR spectra of $[\text{Rh}(\text{Ph}_2\text{PCH}=\text{C}(\text{O})\text{Ph})(\text{CO})(\text{PPh}_3)]$ (**7**) at 295 (A), 240 (B), 230 (C), 220 (D), and 200 K (E).

chemically different phosphorus atoms indicates that PPh_3 is coordinated *trans* to the other phosphorus atom (see Figure 3). The spectrum at 295 K contains a doublet for the phosphino enolate ligand and a broad resonance for PPh_3 and no coupling between them. The disappearance of the coupling between rhodium and PPh_3 indicates partial dissociation (Scheme 3) with formation of a 14-electron species. Heating of the solution led to further broadening and decomposition. The coalescence temperature for this dynamic process was estimated from the Eyring equation as 43.4 ± 0.9 kJ

mol^{-1} .¹⁸ We have checked that the disappearance of the $^1J(\text{RhP})$ coupling is not due to exchange with an excess of phosphine ligand by washing a sample of **7** thoroughly with ether, in which PPh_3 is soluble, before recording the spectrum. PPh_3 dissociation occurs in benzene, toluene/THF, or CH_2Cl_2 solutions (eq 1).



Reactions with $[\text{Rh}(\mu\text{-Cl})(\text{COE})_2]_2$ under Carbon Monoxide. When $[\text{Rh}(\mu\text{-Cl})(\text{COE})_2]_2$ (COE = cyclooctene) and 4 equiv of keto phosphine were reacted in toluene under a carbon monoxide atmosphere $[\text{RhCl}(\text{CO})(\text{P}\sim\text{O})_2]$ (**8**) was isolated (Scheme 3). Analytical and spectroscopic data are in agreement with the structure drawn and the coordination of two monodentate phosphine ligands. The *trans* position of the phosphorus atoms in **8** was inferred from the $J(\text{RhP})$ value of 128 Hz, close to values observed for **5** and **6**.

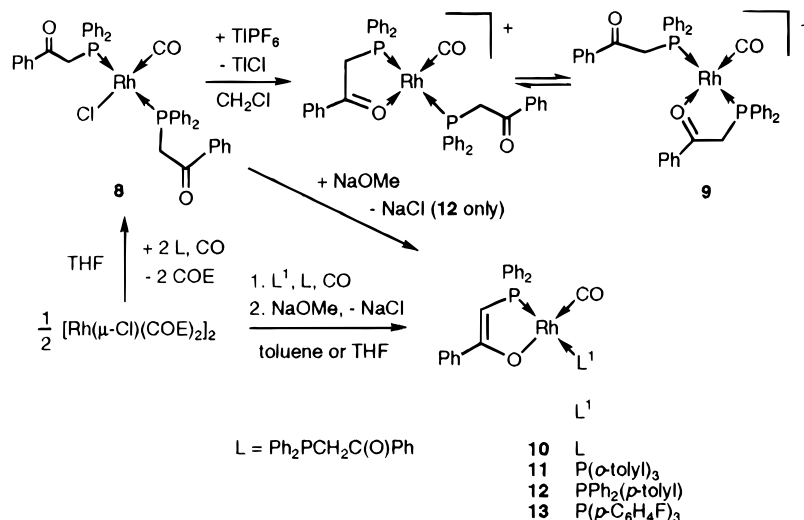
Reaction of this complex with 1 equiv of TIPF_6 in CH_2Cl_2 gave the cationic complex $[\text{Rh}(\text{CO})(\text{P}\sim\text{O})(\text{P}\sim\text{O})][\text{PF}_6]$ (**9**), in which one of the keto phosphines is terminal and the other chelating (IR absorptions at 1678 and 1561 cm^{-1} , respectively). The $^{31}\text{P}\{^1\text{H}\}$ NMR spectrum at 295 K consists of a doublet at 32.5 ppm with $J(\text{RhP}) = 128$ Hz. The ^1H NMR spectrum at room temperature contains a triplet, which broadened on cooling to 180 K without reaching coalescence. This is indicative of a dynamic behavior during which the two keto oxygen donors compete for a common coordination site, *cis* to the P atoms (Scheme 3).

Similarly to the formation of the phosphino enolate complex **7**, reaction of a THF solution of **8** with 1 equiv of sodium methoxide in methanol quantitatively afforded $[\text{Rh}\{\text{Ph}_2\text{PCH}=\text{C}(\text{O})\text{Ph}\}(\text{CO})(\text{P}\sim\text{O})]$ (**10**) (Scheme 3). The usefulness of complexes similar to **7** in transfer dehydrogenation (see below) led us to develop a one-pot synthesis starting from $[\text{Rh}(\mu\text{-Cl})(\text{COE})_2]_2$. Addition of keto phosphine **L** and phosphine L^1 under a CO atmosphere afforded neutral intermediates similar to **5**, as shown by IR spectroscopy ($\text{L}^1 = \text{PPh}_2(p\text{-tolyl})$), $\nu(\text{C}\equiv\text{O})$ 1973 cm^{-1} and $\nu(\text{C}=\text{O})$ 1672 cm^{-1} , which on addition of sodium methoxide yielded the pure phosphino enolato complexes **11–13**. These reactions are summarized in Scheme 3.

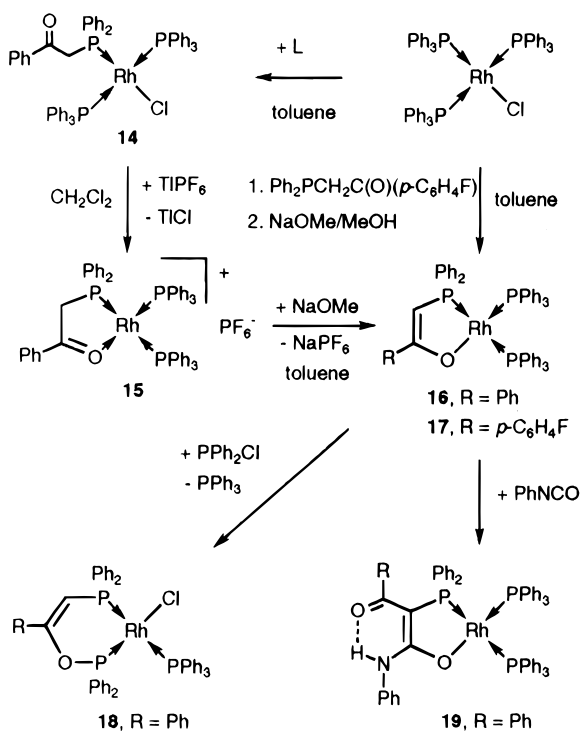
Interestingly for the phosphino enolato carbonyl complexes **7** and **10–13** the carbonyl stretching frequency is independent of the nature of the phosphine ligand L^1 . This can be ascribed to extensive electron delocalization within the enolate system, which redistributes the electron density through the whole complex. Consistently, the enolate absorption band and the chemical shift value of the enolate proton are also independent of L^1 . The value for the carbonyl stretch between 1956 and 1961 cm^{-1} indicates a higher electron density on the rhodium center than that in $[\text{RhCl}(\text{CO})(\text{PPh}_3)_2]$ (1975 cm^{-1}) but is comparable to that in $[\text{RhCl}(\text{CO})(\text{PMe}_3)_2]$ (1956 cm^{-1}).

Reactions with $[\text{RhCl}(\text{PPh}_3)_3]$. The reactivity of the keto phosphine **L** toward $[\text{RhCl}(\text{PPh}_3)_3]$ and subsequent reactions are very similar to those with $[\text{RhCl}$

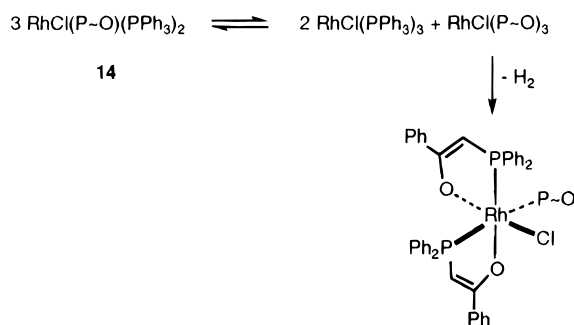
Scheme 3



Scheme 4



Scheme 5



could also be formed by starting from 1 and 2 equiv of PPh_3 (*vide supra*).

When 1 equiv of TIPF_6 was added to **14**, formed *in situ* in acetone/ CH_2Cl_2 , the cationic complex $[\text{Rh}(\text{P}^{\ominus}\text{O})(\text{PPh}_3)_2][\text{PF}_6]$ (**15**) was isolated as red crystals. Analytical and spectroscopic data are in agreement with the structure proposed.

The phosphino enolate complex $[\text{Rh}\{\text{Ph}_2\text{PCH}=\text{C}(\text{O})\text{Ph}\}(\text{PPh}_3)_2]$ (**16**), which was found useful for alkane activation (see below), was obtained by reacting a toluene solution of **14** or a toluene suspension of **15** with 1 equiv of sodium methoxide in methanol. Analytical and spectroscopic data are in agreement with the formulation. In a manner similar to the synthesis of **16** but using $\text{Ph}_2\text{PCH}_2\text{C}(\text{O})(\text{p-C}_6\text{H}_4\text{F})$,

we synthesized $[\text{Rh}\{\text{Ph}_2\text{PCH}=\text{C}(\text{O})(\text{p-C}_6\text{H}_4\text{F})\}(\text{PPh}_3)_2]$ (**17**) (Scheme 4). The ambident character of the enolate moiety in **16** was confirmed in reactions with phenyl isocyanate and chlorodiphenylphosphine. Thus, **16** reacted readily at room temperature with 1 equiv of Ph_2PCl , affording in good yield the complex $[\text{RhCl}\{\text{Ph}_2\text{PCH}=\text{C}(\text{Ph})\text{OPPh}_2\}(\text{PPh}_3)]$ (**18**), which resulted from nucleophilic substitution of the P–Cl bond by the enolate oxygen atom. Reaction of **16** with phenyl isocyanate afforded *cis*- $[\text{Rh}\{\text{Ph}_2\text{C}[\text{C}(\text{O})\text{Ph}]=\text{C}(\text{O})\text{NHPh}\}(\text{PPh}_3)_2]$ (**19**) (Scheme 4). As shown by $^{31}\text{P}\{^1\text{H}\}$ NMR spectroscopy, only one isomer was formed. The ^1H NMR spectra revealed the presence of a signal at δ 10.4 ppm that was assigned to the amide proton after a D_2O –

$(\text{CO})(\text{PPh}_3)_2]$. Addition of 1 equiv of **L** to a toluene solution of $[\text{RhCl}(\text{PPh}_3)_3]$ gave the complex $[\text{RhCl}(\text{PPh}_3)_2(\text{P}^{\ominus}\text{O})]$ (**14**), analogous to **5** (Scheme 4). The $^{31}\text{P}\{^1\text{H}\}$ NMR spectrum of the reaction mixture showed the presence of 1 equiv of free PPh_3 , a doublet of triplets for the keto phosphine, and a doublet of doublets for the two equivalent Rh-bound PPh_3 ligands. IR monitoring of a toluene solution of **14** showed the development within 3 h of a strong band at 1520 cm^{-1} characteristic of a phosphino enolate ligand. The $^{31}\text{P}\{^1\text{H}\}$ NMR spectrum of this toluene solution after 4 days showed the presence of *mer*- $[\text{RhCl}\{\text{Ph}_2\text{PCH}=\text{C}(\text{O})\text{Ph}\}(\text{P}^{\ominus}\text{O})]$ and $[\text{RhCl}(\text{PPh}_3)_3]$. As the reaction of $[\text{RhCl}(\text{PPh}_3)_3]$ with 3 equiv of **L** has been shown to proceed *via* $[\text{RhCl}(\text{P}^{\ominus}\text{O})_3]$ to the rhodium(III) complex *mer*- $[\text{RhCl}\{\text{Ph}_2\text{PCH}=\text{C}(\text{O})\text{Ph}\}_2(\text{P}^{\ominus}\text{O})]$,^{1a} it is likely that phosphine exchange in **14** occurs according to Scheme 5. Note that mixed phosphine complexes such as **14**

Scheme 6

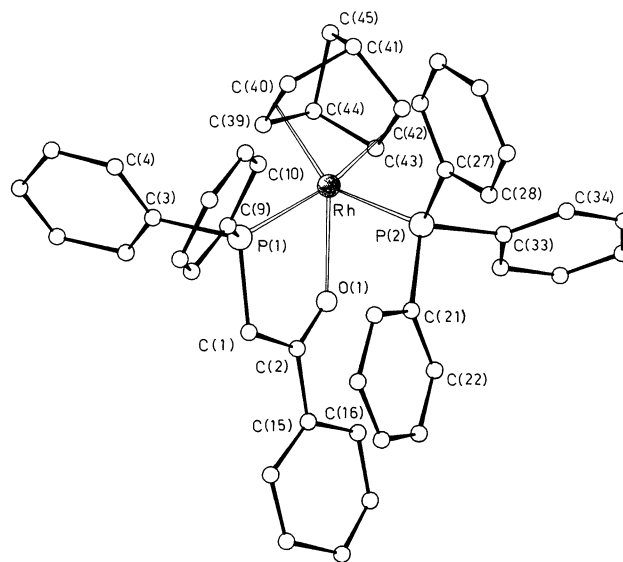
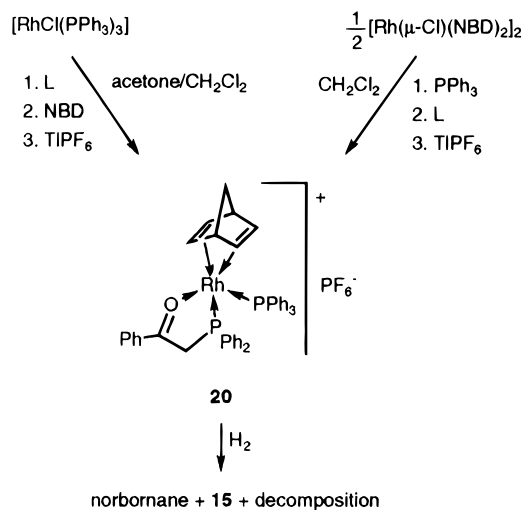


Figure 4. View of the structure of the cationic complex $[\text{Rh}(\text{NBD})(\text{P}^{\ominus}\text{O})(\text{PPh}_3)]^+$ in **20** with the atom-numbering scheme.

NH exchange experiment. This value reflects hydrogen bonding with the oxygen atom of the neighboring carbonyl group, thus forming a stable six-membered ring. In the IR spectrum no $\nu(\text{N-H})$ vibration was detected. Bands appear in the $1550\text{--}1625\text{ cm}^{-1}$ region due to the conjugated ligand system. Although coordination by the nitrogen cannot be ruled out with certainty (with the enolate oxygen atom occupying the place of the NPh group), the high value of 216 Hz for $J(\text{RhP})$ is consistent with a phosphorus *trans* to oxygen, and comparison with previous data²⁷ are in favor of the structure shown in Scheme 4. It results formally from the nucleophilic attack of the carbon atom α to the phosphorus of the phosphino enolate ligand on the carbon atom of PhNCO, followed by a 1,3-hydrogen shift. These reactions are analogous to those previously reported for phosphino enolate complexes such as *cis*-

$[\text{M}\{\text{Ph}_2\text{PCH}_2\text{C}(\text{O})\text{Ph}\}_2]$ ($\text{M} = \text{Ni}, \text{Pd}, \text{Pt}$) with chlorophosphines²⁸ and aryl isocyanates.^{20,29}

When **L**, norbornadiene (NBD), and TlPF_6 were added in sequence to a solution of $[\text{RhCl}(\text{PPh}_3)_3]$ in acetone, orange crystals were isolated in 50% yield. They were shown to be identical with the product obtained from the reaction of PPh_3 , **L**, and TlPF_6 with $[\text{Rh}(\mu\text{-Cl})(\text{NBD})_2]$ (Scheme 6). An unusually high field ^1H NMR signal for the PCH_2 group at 3.03 ppm motivated an X-ray structure analysis, which established the formulation as $[\text{Rh}(\text{NBD})(\text{P}^{\ominus}\text{O})(\text{PPh}_3)]^+[\text{PF}_6]^-$ (**20**) (Figure 4). Although pentacoordinated, this complex is not fluxional in solution in the temperature range 200–330 K. No complex analogous to **20** was obtained in reactions involving 1,5-cyclooctadiene (COD) instead of NBD. This is in agreement with literature data, since no pentacoordinated rhodium complex with COD and monodentate phosphine appears to be known. Whereas the $\nu(\text{C}=\text{O})$ vibration of the coordinated keto group in square-planar and octahedral complexes is generally observed around $1575\text{--}1565\text{ cm}^{-1}$ ($95\text{--}105\text{ cm}^{-1}$ coordination shift), in the pentacoordinated complex **20** it occurs at 1620 cm^{-1} (50 cm^{-1} shift). In the case of the ferrocenyl-substituted keto phosphine $\text{Ph}_2\text{PCH}_2\text{C}(\text{O})(\eta^5\text{-C}_5\text{H}_4)\text{Fe}(\eta^5\text{-C}_5\text{H}_5)$ a

shift of only 35 cm^{-1} was observed upon complexation in the trigonal-planar copper complex $[\text{Cu}(\text{P}^{\ominus}\text{O})(\text{P}^{\ominus}\text{O})]$.³⁰ In a study of cobalt(II) complexes, it has been found that chelation of the keto phosphine ligand is considerably less favored in tetrahedral than in octahedral or square-planar complexes.³¹ Together with the IR shift of the carbonyl stretch upon chelation, this illustrates that the interaction between the carbonyl oxygen of the keto phosphine and a metal markedly depends on the angle of chelation required by the metal orbitals. Octahedral and square-planar geometries are more favorable than trigonal-bipyramidal (in the equatorial plane), tetrahedral, and trigonal-planar ones. Treatment of **20** in toluene with sodium hydride or sodium methoxide led to decomposition. Apparently the pentacoordinated environment is unfavorable for enolate formation from the P,O ligand. Under a hydrogen atmosphere **20** decomposed to **15** (identified by $^{31}\text{P}\{^1\text{H}\}$ NMR), norbornane (detected by GC), and an uncharacterized black precipitate.

Reactions with $[\text{Rh}(\mu\text{-Cl})(\text{COE})_2]_2$, Diene, and Base. Our interest in catalytic studies of rhodium(I)–enolate complexes led us to use diolefin coligands in order to permit isolation. Addition in sequence of an excess of norbornadiene, 1 equiv of **L**, and a slight excess of sodium methoxide to dimeric $[\text{Rh}(\mu\text{-Cl})(\text{COE})_2]_2$ in toluene led to the isolation in high yield of an orange crystalline solid which was analyzed as $[\text{Rh}\{\text{Ph}_2\text{PCH}_2\text{C}(\text{O})\text{Ph}\}(\text{NBD})]$ (**21**). The typical $\nu(\text{C}=\text{O})$ absorption of the keto group in **L** is replaced in **21** by a strong absorption in the range $1520\text{--}1510\text{ cm}^{-1}$, typical for the $\nu(\text{C}=\text{O}) + \nu(\text{C}-\text{C})$ vibration of the enolate system. In a similar manner we synthesized $[\text{Rh}\{\text{R}^1_2\text{PC}(\text{O})\text{R}^2\}(\text{diolfin})]$ (**22–25**) employing **L** and COD (**22**), $\text{Ph}_2\text{PCH}_2\text{C}(\text{O})\text{Me}$ and NBD (**23**), $\text{Ph}_2\text{PCH}_2\text{C}(\text{O})(p\text{-C}_6\text{H}_4\text{F})$ and NBD (**24**), or *i*-Pr₂PCH₂C(O)Ph and

(27) Bouaoud, S.-E.; Braunstein, P.; Grandjean, D.; Matt, D.; Nobel, D. *Inorg. Chem.* **1988**, *27*, 2279.

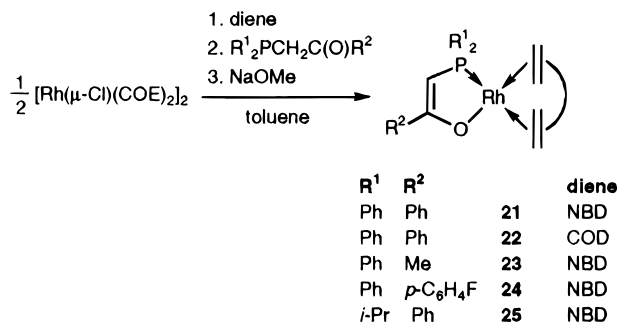
(28) Balegroune, F.; Braunstein, P.; Grandjean, D.; Matt, D.; Nobel, D. *Inorg. Chem.* **1988**, *27*, 3320.

(29) Braunstein, P.; Nobel, D. *Chem. Rev.* **1989**, *89*, 1927.

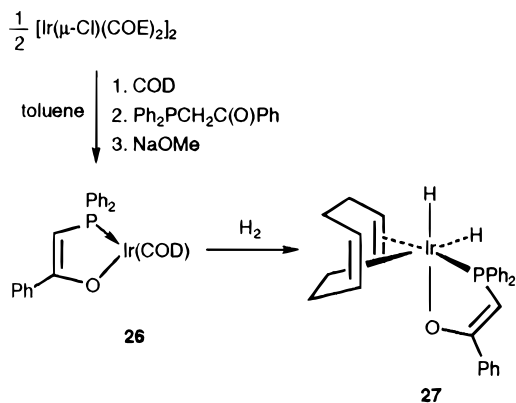
(30) Balegroune, F.; Braunstein, P.; Gomes Carneiro, T. M.; Grandjean, D.; Matt, D. *J. Organomet. Chem.* **1989**, *367*, 117.

(31) Braunstein, P.; Kelly, D. G.; Dusausoy, Y.; Tiripicchio, A. *Inorg. Chem.* **1993**, *32*, 4835.

Scheme 7

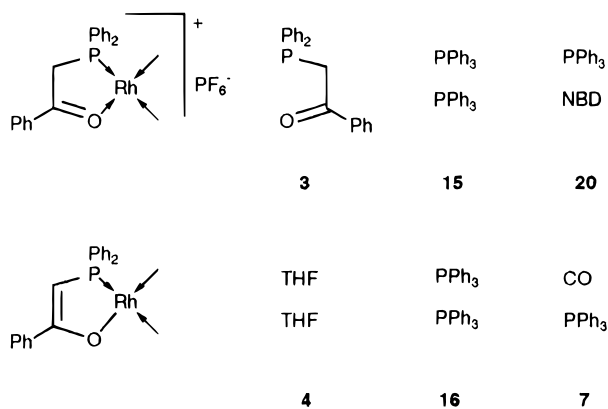


Scheme 8



NBD (**25**) (Scheme 7). These complexes are analogous to the complexes $[\text{Rh}(\text{acac})(\text{diolenin})]$. No high-field ^1H NMR resonance was detected for solutions of complexes **21**–**25** under hydrogen at atmospheric pressure, but at 0.8 MPa the solutions turned progressively black in over 20 min and the olefinic signals disappeared. Thus hydrogenation of coordinated diene was accompanied by decomposition of the 12 electron fragment $[\text{Rh}\{\text{R}^1_2\text{PCH}_2\text{C}(\text{O})\text{R}^2\}]$. The reaction of $[\text{Ir}(\mu\text{-Cl})(\text{COE})_2]_2$ with COD, **L**, and sodium methoxide in toluene yielded $[\text{Ir}\{\text{Ph}_2\text{PCH}_2\text{C}(\text{O})\text{Ph}\}(\text{COD})]$ (**26**). Its characteristic spectroscopic data are similar to those for its rhodium analog **22**. When **26** was placed under an atmosphere of hydrogen, the ^1H NMR spectrum showed two high-field doublets at $\delta -11.03$ ($J(\text{PH}) = 18.1$ Hz) and -18.04 ($J(\text{PH}) = 11.9$ Hz), in contrast to the case of **22**. Chemical shifts and coupling constants are indicative of hydrides *cis* to the phosphorus atom and *trans* to an olefinic double bond and the oxygen atom, respectively. Four signals were found for the chemically inequivalent 1,5-cyclooctadiene vinyl protons due to the lack of symmetry caused by the hydride ligands. These data suggest that the hydride complex $[\text{Ir}\{\text{Ph}_2\text{PCH}_2\text{C}(\text{O})\text{Ph}\}(\text{H})_2(\text{COD})]$ (**27**) was formed (Scheme 8). It was stable for ca. 1 h at room temperature before hydrogenation of the COD ligand occurred. Recently, Oro, Werner, et al. have reported the hydrogenation of alkynes catalyzed by cationic iridium cyclooctadiene phosphino-ether complexes, which under hydrogen are in equilibrium with a cationic hydride complex similar to **27**, as judged by their high-field ^1H NMR data. The latter could be characterized spectroscopically before

Scheme 9



hydrogenation of the coordinated diene took place and a black precipitate was formed.³²

3. Hydrogenation of 1-Hexene Catalyzed by Cationic Keto Phosphine and Neutral Phosphino Enolate Complexes. We examined the reactivity of cationic keto phosphine complexes **3**, **15**, and **20** and neutral phosphino enolate complexes **4**, **7**, and **16** toward 1-hexene at atmospheric pressure. These complexes were chosen for the diversity of ligand sets available (Scheme 9).

Complex **20** in THF hydrogenates and isomerizes 1-hexene catalytically to hexane and only *trans*-2-hexene, respectively. Since isomerization generally involves monohydride complexes, an equilibrium between a cationic dihydride and a neutral monohydride complex is likely to occur. A similar equilibrium has been suggested for cationic rhodium complexes with monodentate phosphine ligands.³³

Under the conditions employed, **3** and **15** were inactive in acetone. Hydrogenation of unsaturated organic substrates with metal complexes which do not contain M–H bonds implies as the initial step the reaction with molecular hydrogen.³⁴ For **3** no hydride was detected under hydrogen. This would be consistent with the electron density at the rhodium center, which is complexed by two relatively hard donor keto groups, being insufficient for oxidative addition of hydrogen to occur. When **15** was placed under hydrogen, no hydride was detected by ^1H NMR and no dissociation of PPh_3 was observed by $^{31}\text{P}\{^1\text{H}\}$ NMR.

All phosphino enolate complexes tested were active hydrogenation and isomerization catalysts. The activity decreased in the order **4** > **16** > **7**, which is also the order of weakly to strongly coordinating ligands (Table 1). Thus, we propose that ligand dissociation leads to the active catalytic species $[\text{Rh}\{\text{Ph}_2\text{PCH}_2\text{C}(\text{O})\text{Ph}\}(\text{L})]$ ($\text{L} = 2e\text{-donor ligand}$) having vacant coordination sites. The isomerization activity suggests an equilibrium between a Rh(III) phosphino enolate dihydride and a Rh(I) keto phosphine monohydride complex.

4. Transfer Dehydrogenation of Cyclooctane with Norbornene Catalyzed by Phosphino Enolate Complexes. The activation of alkanes by soluble transition-metal species has aroused considerable inter-

(32) Esteruelas, M. A.; López, A. M.; Oro, L. A.; Pérez, A.; Schulz, M.; Werner, H. *Organometallics* **1993**, *12*, 1823.

(33) Schrock, R. R.; Osborn, J. A. *J. Am. Chem. Soc.* **1976**, *98*, 2134.

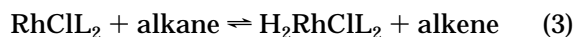
(34) James, B. R. *Homogeneous Hydrogenation*; Wiley: New York, 1973.

Table 1. Hydrogenation and Isomerization of 1-Hexene Catalyzed by Cationic Rhodium Keto Phosphine and Neutral Rhodium Phosphino Enolate Complexes^a

entry no.	complex	solvent	conversion, %	amt of hexane, %	amt of 2- <i>trans</i> -hexene, %	amt of 2- <i>cis</i> -hexene, %
1	4	thf	99.2	44	27	28
2	7	toluene	10	45	43	12
3	16	toluene	50	69	17	14
4	20	thf	85	22	48	30

^a Reaction conditions: 0.8 mol of 1-hexene; 5 mmol of rhodium complex; stirred for 1 h at 300 K; $p(\text{H}_2) = 0.1$ MPa.

est.³⁵ It emerged that the catalyst has to be resistant to dimerization or β -elimination of its ligands, which represent major deactivation pathways.³⁶ [RhCl(CO)(PMe₃)₂] was reported to be the first efficient (>100 turnovers) organometallic alkane functionalization catalyst, effecting photochemical dehydrogenation of alkanes to yield the corresponding alkenes with turnover rates as high as 300/h.³⁷ The proposed mechanism for the catalytic cycle involved photogeneration of the three-coordinate fragment RhL₂Cl (eq 2, L = PMe₃), transfer of hydrogen from the alkane (eq 3), and displacement of H₂ from H₂RhCl(PMe₃)₂ with CO to regenerate RhCl(CO)L₂ (eq 4).



More recently it was found that [RhCl(CO)(PMe₃)₂] also catalyzes thermal dehydrogenation of alkanes to the corresponding alkenes, but exclusively under an atmosphere of dihydrogen. The catalysis is initiated by the reverse of eq 4, and the catalytic cycle consists of eq 3 and its microscopic reverse (where the alkene is a sacrificial hydrogen acceptor). Thermodynamic studies corroborated these findings.³⁸ Also, Miller and Knox reported efficient thermal dehydrogenation of alkanes with [RhCl(AsPh₃)₂]₂ and [RhCl(CO)(AsMe₃)₂] as catalyst precursors under 3.4 MPa of hydrogen at 60–100 °C with turnover rates reaching 600/h.^{9d}

We anticipated that, owing to the ability of complexes **7** and **16** to catalyze hydrogenation of 1-hexene (the reverse reaction of eq 3) and to the facile dissociation of triphenylphosphine from complex **7** in solution (eq 1), phosphino enolate complexes could be good candidates for the catalytic transfer dehydrogenation of alkanes under conditions similar to those used by Goldman. The solubility of the complexes used allows the catalysis to be performed in neat alkane. Two important parameters are turnover frequencies of cy-

(35) (a) Crabtree, R. H. In *The Chemistry of Alkanes and Cycloalkanes*; Patai, S., Ed.; Wiley: New York, 1992; p 653. (b) Crabtree, R. H. *Chem. Rev.* **1985**, *85*, 245.

(36) Crabtree, R. H.; Mellea, M. F.; Mihelcic, J. M.; Quirk, J. M. *J. Am. Chem. Soc.* **1982**, *104*, 107.

(37) (a) Nomura, K.; Saito, Y. *J. Chem. Soc., Chem. Commun.* **1988**, 161. (b) Sakakura, T.; Sodeyama, T.; Tokunaga, M.; Tanaka, M. *Chem. Lett.* **1988**, 263. (c) Maguire, J. A.; Boese, W. T.; Goldman, A. S. *J. Am. Chem. Soc.* **1989**, *111*, 7088. (d) Maguire, J. A.; Boese, W. T.; Goldman, M. E.; Goldman, A. S. *Coord. Chem. Rev.* **1990**, *97*, 179.

(38) Wang, K.; Rosini, G. P.; Nolan, S. P.; Goldman, A. S. *J. Am. Chem. Soc.* **1995**, *117*, 5082.

Table 2. Transfer Dehydrogenation of Cyclooctane with Norbornene Catalyzed by Rhodium Carbonyl Phosphino Enolate Complexes: Effect of Aromatic Phosphines

entry no. ^a	L ¹ <i>trans</i> to phosphino enolate	turnover freq		K
		mol of COE (mol of Rh) ⁻¹ h ⁻¹	mol of NBA (mol of Rh) ⁻¹ h ⁻¹	
1	PPh ₃	230	2200	0.10
2	PPh ₂ (<i>p</i> -tolyl)	180	2200	0.08
3	P(<i>p</i> -C ₆ H ₄ F) ₃	130	860	0.15
4 ^b	P(<i>p</i> -C ₆ H ₄ F) ₃	115	1250	0.1

^a Reaction conditions: 333 K; 20 mL of COA; 1.9 M NBE; 0.4 mM Rh complex; $p(\text{H}_2) = 7$ MPa. ^b Catalyst in entry 3 reused after elimination of reactants and products; 323 K.

Table 3. Transfer Dehydrogenation of Cyclooctane with Norbornene Catalyzed by Rhodium Carbonyl Enolate Complexes: Effect of Various Phosphines

entry no. ^a	L ¹ <i>trans</i> to phosphino enolate	turnover freq		K
		mol of COE (mol of Rh) ⁻¹ h ⁻¹	mol of NBA (mol of Rh) ⁻¹ h ⁻¹	
5	PPh ₃	370	7000	0.054
6	PMe ₃ ^b	10	1700	0.006
7	P~O	7	4700	0.001
8	P(<i>o</i> -tolyl) ₃	0	3600	0

^a Reaction conditions: 363 K; 20 mL of COA; 3.4 M NBE; 0.4 mM Rh complex; $p(\text{H}_2) = 7$ MPa. ^b Preparation of [Rh(Ph₂PC-

H₂C(-O)Ph](CO)(PMe₃)]₄: [AgI(PMe₃)₄] (0.04 mmol) was heated to 200 °C, and the PMe₃ thus liberated was condensed into a frozen yellow solution of **7** (0.098 g, 0.14 mmol) in toluene (10 mL). When it was stirred at room temperature, the solution rapidly became orange. Concentration, addition of pentane (40 mL), and cooling to -20 °C precipitated a cream-yellow solid, which was isolated by filtration (0.057 g) but not fully characterized (IR showed it to contain no carbonyl ligand). Evaporation of the yellow filtrate gave orange crystals of the product, which were filtered and washed with a small amount of pentane (0.046 g, 64%). IR (C₆D₆): 1961 vs $\nu(\text{C}=\text{O})$, 1516 s $\nu(\text{C}=\text{O}) + \nu(\text{C}=\text{C})$ cm⁻¹. ¹H NMR (C₆D₆): δ 8.1–7.25 (15H, m, Ph), 5.33 (1H, s, PCH), 1.10 (9H, s, 3 Me).

clooctene (COE) and norbornene (NBA) formation and the COE/NBA molar ratio (*K*), whose ideal value is 1.

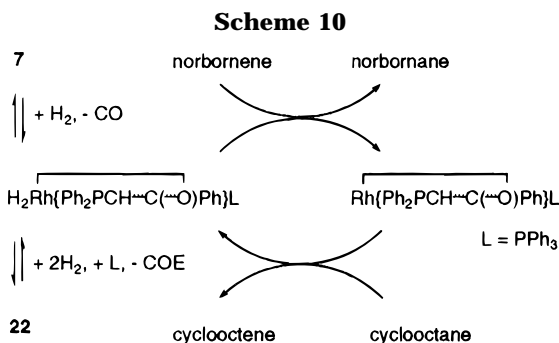
The results obtained using complexes **7**, **12**, and **13** are given in Table 2. The *K* value increases slightly in the order PPh₂(*p*-tolyl) < PPh₃ < P(*p*-C₆H₄F)₃ (entries 2, 1, and 3), with decreasing phosphine basicity. This observation cannot be rationalized on the basis of an oxidative-addition character of the alkane C–H bond activation, which has been mentioned before (*vide infra*).^{35b,39} This is further supported by the observation that when the more basic PMe₃ was used as the L¹ ligand (entry 6, Table 3) only hydrogenation took place. The potentially chelating keto phosphine Ph₂PCH₂C(O)Ph (entry 7) considerably decreased the dehydrogenation reaction. The complete inactivity of the tri-*o*-tolylphosphine-based enolate complex (entry 8) could be ascribed to a cyclometalation side reaction.⁴⁰ Cyclometalation has been mentioned as limiting catalyst activity by providing a pathway for catalyst deactivation,^{9c,41} and alkane activation is especially sensitive to it.⁴² Changing the solution volume (20 or 40 mL in a 100 mL reactor) did not affect *K*.⁴³

(39) Another possibility would be that dissociation of the tri-arylphosphine may precede the approach of the alkane.

(40) Cheney, A. J.; Shaw, B. L. *J. Chem. Soc., Dalton Trans.* **1972**, 754, 860.

(41) Garrou, P. *Chem. Rev.* **1985**, *85*, 171.

(42) Burk, M. J.; Crabtree, R. H. *J. Am. Chem. Soc.* **1987**, *109*, 8025.



The catalyst could be recycled after removal of reactants and products by vaporization under vacuum (Table 2, entries 3 and 4). Accordingly, IR spectra of reaction solutions of **7** and **13** after catalysis revealed no decrease of the characteristic carbon monoxide stretch at 1960 cm⁻¹ and of the enolate stretch at 1515 cm⁻¹. The ¹H NMR spectrum in CD₂Cl₂ solution showed a peak at 4.75 ppm which was attributed to the enolate proton. The solution remains homogeneous, and catalysis is unaffected by the addition of mercury to the reaction mixture, implying that the active catalytic species is not colloidal.⁴⁴ In fact, the reaction is limited by complete hydrogenation of the hydrogen acceptor, not by catalyst decomposition. Accordingly, we found no trace of benzene (GC) which could have resulted from phosphorus-phenyl bond hydrogenolysis.

To investigate the fate of the catalyst precursor, an experiment was carried out with complex **13** under deuterium. ¹H NMR analysis of complex **13** after several hundred turnovers still showed a peak for the enolate proton, suggesting that the P,O ligand was only present in the enolate form throughout the catalytic cycle (absence of deuterated enolate). An equivalent amount of norbornane-*d*₀ and dehydrogenated cycloalkane was found by GC-MS. The presence of norbornane-*d*₂ and the absence of cyclooctane-*d*₂ shows the selective hydrogenation of norbornene in the presence of cyclooctene. No monodeuterated alkanes or olefins were detected, indicating that the transfer of hydrogen takes place exclusively via dihydride complexes, consistent with the propensity of Rh(I) to form dihydride complexes.^{44,45}

Our results with phosphino enolato carbonyl complexes are consistent with [Rh{Ph₂PCH=C(O)Ph}L¹] being a key intermediate in the catalytic cycle (see Scheme 10). The *K* values published for [RhCl(CO)(PMe₃)₂] are in the range 0.16–0.29 using cyclooctane and various olefins as substrates, and [RhCl(PMe₃)₂] was identified as the catalytically active fragment.^{9a} Interestingly, the carbonyl infrared stretching frequencies for **7** (1960 cm⁻¹) and for [RhCl(CO)(PMe₃)₂] (1956 cm⁻¹) are similar. For the transfer dehydrogenation of alkanes under hydrogen pressure with [RhCl(AsPh₃)₂]₂ and [RhCl(CO)(AsMe₃)₂] as catalyst precursors, no *K* values were published.^{9d} The common denominator of the three systems appears to be the involvement of the d⁸ three-coordinate fragment [RhXL₂]. The class of

Table 4. Transfer Dehydrogenation of Cyclooctane with Norbornene Catalyzed by Complex **13: Effect of Addition of Trimethylamine Oxide**

entry no. ^a	catalyst precursor	turnover freq		<i>K</i>
		mol of COE (mol of Rh) ⁻¹ h ⁻¹	mol of NBA (mol of Rh) ⁻¹ h ⁻¹	
9	13	210	4500	0.046
10	13 + 0.6 equiv of ONMe ₃	880	18500	0.047

^a Reaction conditions: 363 K; 20 mL of COA; 3.4 M NBE; 0.4 mM Rh complex; *p*(H₂) = 7 MPa.

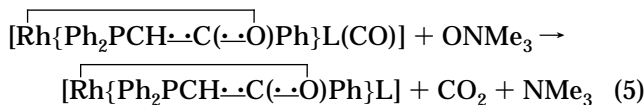
Table 5. Transfer Dehydrogenation of Cyclooctane with Norbornene Catalyzed by Complex **22: Effect of Addition of Triphenylphosphine**

entry no. ^a	PPh ₃ /Rh molar ratio	turnover freq		<i>K</i>
		mol of COE (mol of Rh) ⁻¹ h ⁻¹	mol of NBA (mol of Rh) ⁻¹ h ⁻¹	
11	0	10	1000	0.01
12	0.5	100	1700	0.06
13	1	80	740	0.11
14	1.8	7	260	0.03
15 ^b	1	25	490	0.05

^a Reaction conditions: 343 K; 20 mL of COA; 1.9 M NBE; 0.4 mM Rh complex; *p*(H₂) = 0.1 MPa. ^b Complex **23**; 298 K.

compounds MXL₂, with M being a d⁸ metal, has indeed been cited as promising for alkane activation.³⁵

Accordingly, addition of 0.6 equiv of amine oxide ONMe₃ to the enolate complex **13** considerably increased the reaction rates (Table 4, entry 10). This can be ascribed to the elimination of carbon monoxide from the complex (eq 5).⁴⁶ Addition of more than 1 equiv of amine oxide resulted in a decrease of the reaction rates, probably due to partial oxidation of rhodium. The *K* value was unchanged.



This led us to investigate phosphino enolate complexes containing no carbon monoxide ligand. The fragment [Rh{Ph₂P{CH=C(O)Ph}L¹}] can be easily accessed from **22** and L¹ under an hydrogen atmosphere, thus allowing great flexibility in the choice of L¹ (Scheme 10). Table 5 gives the results obtained with **22** after addition of various amounts of PPh₃. As observed by Goldman *et al.* in the case of [RhCl(PMe₃)₂-(PR₃)] (R = *i*-Pr, Cy, Me),^{9b} the absence of carbon monoxide in the rhodium phosphino enolate complex allowed work at atmospheric pressure. Under catalytic conditions the hydrogen consumption started after an induction period of 13–50 min and was accompanied by a color change from yellow to dark orange. Without

(46) This is in contrast to the previously observed catalytic isomerization of hexene with **7** in toluene (see above). The lower polarity of the cyclooctane/norbornane solvent compared to that of toluene may suppress the formation of monohydride species.

(47) Further comparison of these catalytic systems is fraught with difficulties due to their different behavior on changing reaction conditions, as exemplified by the greater sensitivity to the solution volume of [RhCl(CO)(PMe₃)₂] compared to **7** or to a change in the olefin acceptor.

(48) Albers, M. O.; Coville, N. J. *Coord. Chem. Rev.* **1984**, *53*, 227.

(43) For [RhCl(CO)(PMe₃)₂] the rate decreased with an increasing ratio of solution to gas phase volume.

(44) Anton, D. R.; Crabtree, R. H. *Organometallics* **1983**, *2*, 855.

(45) Sheridan, P. S. In *Comprehensive Coordination Chemistry*; Wilkinson, G., Gillard, R. D., McCleverty, J. A., Eds.; Pergamon Press: Oxford, England, 1987; Vol. 4, p 901.

Table 6. Transfer Dehydrogenation of Cyclooctane with Norbornene Catalyzed by Rhodium and Iridium Phosphino Enolate Complexes: Effect of Various Enolates and Added Ligands

entry no. ^a	complex	L ¹ added	turnover freq		K
			mol of COE (mol of Rh) ⁻¹ h ⁻¹	mol of NBA (mol of Rh) ⁻¹ h ⁻¹	
16	24	PPh ₃	70	1170	0.06
17	25	PPh ₃	1	160	0.004
18	26	PPh ₃	0	300	0
19	26	P(<i>p</i> -tolyl) ₃	1	260	0.003

^a Reaction conditions: 323 K; 20 mL of COA; 2 M NBE; 1 mM enolate metal complex; *p*(H₂) = 0.1 MPa.

any added phosphine, C–H activation was inefficient (entry 11). Adding 1 equiv of triphenylphosphine improved both the stability and the selectivity of the catalyst (entry 13). With less than 1 equiv, the catalyst was still unstable (entry 12), whereas more than 1 equiv strongly inhibited the rates of dehydrogenation and hydrogenation (entry 14). The NBD complex **23** reacted even after 18 min at 25 °C (entry 15) and showed the same color changes. This induction period probably indicates that the phosphino enolate chelate favors a square-planar geometry over a pentacoordinated geometry (see reactivity of **20**). The latter is required in the transition state for H–H addition. A much faster hydrogenation of coordinated NBD versus COD has been observed for cationic Rh(I) phosphine complexes.³³

The results obtained with rhodium complexes **24** and **25** derived from (diphenylphosphino)-*p*-fluoroacetophenone and (diisopropylphosphino)acetophenone (entries 16 and 17) and with iridium complex **26** are presented in Table 6. Complex **24** (entry 16) was as efficient as **22**. With complex **25** no hydrogen transfer occurred (entry 17), presumably due to a cyclometalation side reaction of the isopropyl group similar to that observed by Goldman and Shih in the dehydrogenation of cyclooctane with [RhCl(P-*i*-Pr₃)₂] in the absence of any hydrogen acceptor.^{9c} This suspected cyclometalation reaction could lead to inactive species in catalytic C–H activation. A lower activity of *P*-*i*-Pr₃ compared to PPh₃ has been reported by Tanaka *et al.* on dehydrogenation of cyclooctane with [RhCl(CO)(PR₃)₂] under irradiation.⁴⁹ Arylphosphines are suitable ligands because they cannot decompose by β -elimination.

The iridium complex **26**, analogous to **22**, was quite unreactive for dehydrogenation (entries 18 and 19). A striking difference in H–H activation between rhodium and iridium has been previously observed for [M(COD)L₂]⁺A⁻ (M = Rh, Ir; L = PR₃; A⁻ = BF₄⁻, PF₆⁻, ClO₄⁻) as hydrogenation catalyst precursor for hindered olefins in chlorinated solvents. Iridium was found to be much more active than rhodium.⁵⁰ However, the greater stability of iridium hydride diene complexes allowed the spectroscopic characterization of **27**, an intermediate before entrance into the catalytic cycle. The shorter induction period together with the slower hydrogenation rate of iridium as compared to rhodium is indicative of an easier H₂ addition with iridium and

(49) Sakakura, T.; Sodeyama, T.; Tanaka, M. *New J. Chem.* **1989**, 13, 737.

(50) Crabtree, R. H.; Demou, P. C.; Eden, D.; Mihelcic, J. M.; Parnell, C. A.; Quirk, J. M.; Morris, G. E. *J. Am. Chem. Soc.* **1982**, 104, 6994.

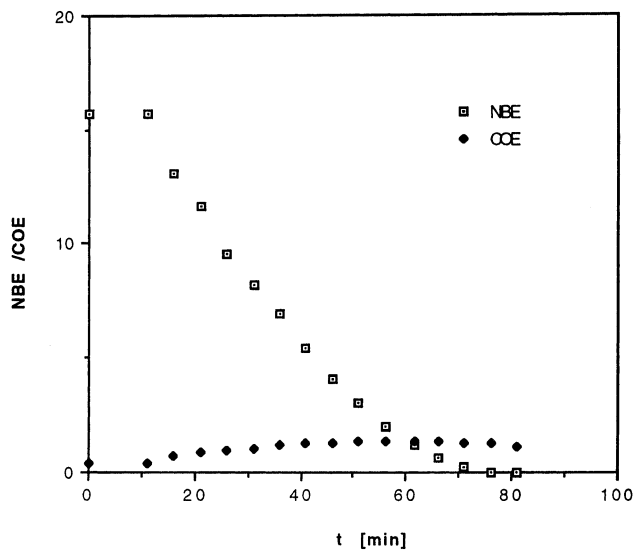


Figure 5. Variation of the norbornene (NBE) and cyclooctene (COE) concentrations with time during a catalytic experiment using **23** and 0.5 equiv of PPh₃.

Table 7. Transfer Dehydrogenation of Cyclooctane Catalyzed by Complex **22: Effect of the Hydrogen Acceptor**

entry no. ^a	hydrogen acceptor	turnover freq		K
		mol of COE (mol of Rh) ⁻¹ h ⁻¹	mol of alkane (mol of Rh) ⁻¹ h ⁻¹	
20	norbornene	80	740	0.11
21	cyclohexene	100	1900	0.05
22	neohexene	30	330	0.09

^a Reaction conditions: 343 K; 20 mL of COA; 1.9 M hydrogen acceptor; 0.4 mM Rh complex; *p*(H₂) = 0.1 MPa.

greater stability of the Ir–H bond compared to Rh–H in these complexes.

Some Mechanistic Considerations. An intriguing feature of both Goldman's and our systems is that an alkane can coordinate to the rhodium center *in the presence* of strongly coordinating norbornene. Accordingly, monitoring hydrogenation/dehydrogenation reactions at various time intervals revealed that, even at high conversion of norbornene, cyclooctene is still unreactive toward hydrogenation (Figure 5).

Under catalytic conditions the rhodium fragment [Rh{Ph₂PCH=C(O)Ph}L¹] may react by three different routes: (1) the dihydride route beginning with addition of H–H, (2) the unsaturated route starting with coordination of a C=C bond, and (3) the alkane route starting with addition of a C–H bond. A concerted mechanism involving simultaneous coordination of alkane and olefin can also be envisioned. Thus, cyclohexene was revealed to be a slightly less favorable hydrogen acceptor than norbornene (Table 7, entry 21), whereas *tert*-butylethylene was less reactive, owing to steric hindrance. However, the *K* value was not very different. This could favor a mechanism where alkane oxidative addition precedes the approach of the olefin, because C–H bond addition in a concerted mechanism would be hindered due to the size of the *tert*-butylethylene. Complex **22** is also less sensitive to the steric bulk of the hydrogen acceptor than Goldman's catalyst [RhCl(PMe₃)₂L¹]. Catalytic alkane dehydrogenation by [IrClH₂(P-*i*-Pr₃)₂] has recently been discussed in terms

Table 8. Crystal Data and Data Collection Parameters^a

	3·H ₂ O	6	20
formula	C ₄₀ H ₃₆ O ₃ F ₆ P ₃ Rh	C ₃₉ H ₃₂ F ₆ O ₂ P ₃ Rh	C ₄₅ H ₄₀ F ₆ OP ₃ Rh
fw	874.5	842.50	906.63
cryst system	triclinic	monoclinic	tetragonal
space group	<i>P</i> $\bar{1}$	<i>P</i> 2 ₁ / <i>a</i>	\bar{I}
cryst dimens, mm	0.24 × 0.24 × 0.06	0.25 × 0.25 × 0.30	0.22 × 0.30 × 0.40
cryst color and habit	red	yellow	orange
<i>a</i> , Å	10.398(3)	16.238(6)	27.453(8)
<i>b</i> , Å	11.159(3)	19.951(8)	27.453(8)
<i>c</i> , Å	17.995(5)	11.411(6)	12.311(3)
α , deg	107.53(2)		
β , deg	102.86(2)	95.15(2)	
γ , deg	84.81(2)		
<i>V</i> , Å ³	1940.4(8)	3694(3)	9278(4)
<i>Z</i>	2	4	8
ρ_{calcd} , g/mL	1.497	1.515	1.298
<i>F</i> (000)	888	1704	3696
diffractometer	Enraf-Nonius CAD4F	Philips PW 1100	Philips PW 1100
linear abs coeff μ , cm ⁻¹	6.177	6.44	5.16
2 θ range, deg	4–48	6–54	6–54
octants collected	$\pm h, \pm k, +l$	$\pm h, k, l$	h, k, l
no. of data collected	6820	7792	8540
no. of unique data used, <i>N</i>	4415	3097	4192
<i>R</i> (<i>R</i> _w)	0.047 (0.072)	0.036 (0.037)	0.059 (0.062)
GOF ^b	1.476	1.108	0.972

^a Details in common: *T* = 295 K; Mo K α graphite-monochromated radiation (λ = 0.710 73 Å); $\theta/2\theta$ scan mode; $(\theta - 0.6) - (\theta + 0.6) + 0.346 \tan \theta$ scan width; 2.5–12°/min scan speed; for complexes **7** and **22**, one standard reflection measured after 75 reflections. ^b GOF = $[\sum w(|F_o| - |F_c|)^2 / (N_{\text{observns}} - N_{\text{params}})]^{1/2}$.

of an alkane association mechanism occurring after olefin insertion into a Ir–H bond.^{51a}

The need for hydrogen as a third reagent, in addition to olefin and alkane, suggests that hydrogen is not merely generating the active species but is directly involved in the catalytic cycle. To test this hypothesis, we generated the active species by hydrogenation. We observed catalytic cyclooctene formation under a hydrogen atmosphere, which stopped under an atmosphere of argon and restarted under hydrogen. As a hypothesis, it could be suggested that dihydrogen plays the role of a particular ligand which, unfortunately, reacts with olefin.

Kinetic experiments show that during a catalytic run the *K* value decreases slightly with decreasing concentration of the acceptor olefin.^{51b} It is not yet clear whether this is due to (i) the hydrogenation “side” reaction, the rate of which is known to be dependent on olefin concentration, (ii) a concerted mechanism involving simultaneous coordination of alkane and olefin, or (iii) deactivation of the catalyst. However, we did not detect benzene in the solution after catalysis which could have resulted from P–C bond hydrogenolysis. Indeed, the rather low temperatures at which the reactions were performed could prevent this deactivation reaction from proceeding at a significant rate.

These results support the view that the 14-electron fragment Rh{Ph₂PCH₂–C(=O)Ph}L¹, (L¹ = phosphine) could be the active catalyst for hydrogen transfer from the alkane. Catalytic transfer dehydrogenation of cyclooctane has now been reported with rhodium complexes bearing three types of ligands: phosphines, arsines, and phosphino enolates. The activation of an aliphatic C–H bond by these quite different ligand systems makes further developments look promising.

5. Discussion of the Crystal Structures. [Rh(P⁺O)₂][PF₆]·H₂O (3·H₂O) (A.D., J.F.).

(51) (a) Belli, J.; Jensen, C. M. *Organometallics* **1996**, *15*, 1532. (b) Braunstein, P.; Chauvin, Y.; Nöhling, J. Unpublished results.

Table 9. Selected Bond Distances (Å) and Angles (deg) for 3·H₂O

Rh–P1	2.182(2)	Rh–P2	2.182(2)
P1–C1	1.861(7)	P2–C21	1.840(7)
C1–C2	1.495(9)	C21–C22	1.499(9)
C2–O1	1.248(7)	C22–O2	1.236(7)
Rh–O1	2.103(4)	Rh–O2	2.104(4)
P1–Rh–O1	83.8(1)	P2–Rh–O2	82.8(1)
Rh–P1–C1	103.1(2)	Rh–P2–C21	100.7(2)
P1–C1–C2	110.1(5)	P2–C21–C22	109.9(4)
C1–C2–O1	121.1(6)	C21–C22–O2	119.1(6)
Rh–O1–C2	121.9(4)	Rh–O2–C22	121.6(4)
P1–Rh–P2	104.39(7)		

graphic data are summarized in Table 8. The molecular structure is shown in Figure 1 together with the atom-numbering scheme; selected bond distances and angles are given in Table 9. The crystal structure consists of discrete [Rh(P⁺O)₂]⁺ cations, [PF₆][–] anions, and water molecules separated by normal van der Waals contacts (the nearest contact of the water molecule is with another one at 2.908 Å, through hydrogen bonding). The Rh center has a square-planar geometry, slightly distorted toward tetrahedral with the phosphorus atoms P1, P2 (and oxygen atoms O1, O2) in a *cis* arrangement and on opposite sides of the mean plane through them and the Rh center (distances to this plane 0.060, –0.0588 Å and –0.0767, 0.0788 Å, respectively). The two chelating keto phosphine ligands have the same geometry and similar bond lengths and angles. The bite angles P1–Rh–O1 and P2–Rh–O2 of 83.8(1) and 82.8(1)°, respectively, are in the normal range. The Rh–P distance of 2.182(2) Å compares well with the average value for Rh–P (2.16 Å) in [Rh(η^4 -{(η^5 -C₅H₄)OCH₂CH₂-PPh₂})₂Fe][BF₄].²³ The Rh–O distances of 2.103(4) and 2.104(4) Å are smaller than Rh–O in the above-cited phosphine–ether complex (average 2.19 Å), indicating stronger bonding to the metal of the keto function than of the ether group.

[Rh(CO)(P⁺O)(PPh₃)] [PF₆] (**6**) (A.T., F.U.). Crystallographic data are summarized in Table 8. A view of the structure of complex **6** is shown in Figure 2

Table 10. Selected Bond Distances (Å) and Angles (deg) for **6**

Rh-P1	2.281(3)	Rh-P2	2.343(3)
P1-C1	1.842(6)	Rh-C3	1.788(7)
C1-C2	1.505(9)	P2-C22	1.814(6)
O1-C2	1.252(6)	P2-C28	1.812(6)
Rh-O1	2.084(4)	P2-C34	1.816(6)
P1-C4	1.814(7)	O2-C3	1.144(9)
P1-C10	1.823(6)	C2-C16	1.451(8)
P1-Rh-O1	82.1(1)	P1-Rh-C3	93.5(2)
P2-Rh-C3	94.8(3)	P2-Rh-O1	89.1(1)
Rh-P1-C1	100.3(2)	Rh-P1-C4	121.6(2)
P1-C1-C2	111.6(4)	Rh-P1-C10	116.7(2)
O1-C2-C1	118.3(5)	Rh-P2-C22	112.1(2)
Rh-O1-C2	124.7(3)	Rh-P2-C28	105.3(2)
O1-C2-C16	119.2(5)	Rh-P2-C34	123.1(2)
C1-P1-C4	106.1(3)	Rh-C3-O2	176.5(6)
C1-P1-C10	105.9(3)	C1-C2-C16	122.5(5)
C4-P1-C10	104.8(3)	C22-P2-C28	105.7(3)
C22-P2-C34	102.4(3)	C28-P2-C34	106.9(3)

together with the atom-numbering scheme; selected bond distances and angles are given in Table 10. The Rh atom displays a slightly distorted square planar coordination involving a phosphorus atom from the PPh₃ ligand (Rh-P2 = 2.343(3) Å), a carbon atom from a terminal carbonyl group (Rh-C3 = 1.788(7) Å), and the phosphorus and the oxygen atoms from the chelating Ph₂PCH₂C(O)Ph ligand (Rh-P1 = 2.281(3) Å and Rh-O1 = 2.084(4) Å). The chelating ligand forms a five-membered ring with the metal in which the P-C-C-O moiety is roughly planar and the Rh atom deviates remarkably from the mean plane passing through the four atoms (0.331(2) Å). The bite angle, 82.1(1)°, is comparable to those found in octahedral Rh(III), Co(III), and Ru(II) complexes with the same ligand (in the 82.0–82.6° range).^{1,31} The values of the C1-C2 and C1-P1 bond distances in the chelate ring (1.505(9) and 1.842(6) Å) are in agreement with single-bond character and that of the C2-O1 bond (1.252(6) Å) with an appreciable double-bond character.

[Rh(NBD)(P^ˆO)(PPh₃)] [PF₆] (20**) (A.T., F.U).** A view of the structure of complex **20** is shown in Figure 4 together with the atom-numbering scheme; selected bond distances and angles are given in Table 11. The Rh center can be considered five-coordinate if the M1 and M2 midpoints of the two olefinic bonds of the NBD ligand are taken as coordination sites (Rh-M1 = 2.127(11) Å and Rh-M2 = 1.998(11) Å). The coordination also involves the P atom from the PPh₃ ligand (Rh-P2 = 2.406(4) Å) and the phosphorus and the oxygen atoms from the chelating Ph₂PCH₂C(O)Ph ligand (Rh-P1 = 2.272(4) Å and Rh-O1 = 2.402(4) Å). The Rh-O distance is much longer than those in **3** or **6**. The geometry around the Rh atom can be described as intermediate between square pyramidal (with the O atom occupying the apical position) and trigonal pyramidal (with P1 and M1 occupying the apical positions), both severely distorted. The chelating ligand forms with the metal a five-membered ring in which the P-C-C-O moiety is roughly planar and the Rh atom deviates remarkably from the mean plane passing through the four atoms (0.557(2) Å). The bite angle of 76.9(2)° is narrower than those of 82.0–82.6° found in square-planar **3** and **6** or octahedral Rh(III) and Ru(II) complexes. The C1-C2 and C1-P1 bond distances in the chelating ligand of 1.529(16) and 1.853(12) Å are practically equal to those found in **6**, whereas the C2-O distance of 1.223(14) Å is significantly shorter.

Table 11. Selected Bond Distances (Å) and Angles (deg) for **20^a**

Rh-P1	2.272(4)	Rh-P2	2.406(4)
Rh-O	2.402(9)	Rh-M1	2.127(11)
P1-C1	1.853(12)	Rh-M2	1.998(11)
P1-C3	1.819(11)	P1-C9	1.811(12)
O-C2	1.223(14)	P2-C21	1.836(11)
P2-C27	1.827(12)	P2-C33	1.840(11)
C1-C2	1.53(2)	C2-C15	1.48(2)
C39-C40	1.38(2)	C42-C43	1.37(2)
C40-C41	1.54(2)	C41-C42	1.52(2)
C39-C44	1.54(2)	C43-C44	1.46(2)
C41-C45	1.53(2)	C44-C45	1.55(2)
M1-Rh-M2	68.7(4)	O-Rh-M2	126.0(4)
O-Rh-M1	104.1(4)	P2-Rh-M2	146.1(3)
P2-Rh-M1	98.6(3)	P2-Rh-O	87.1(2)
P1-Rh-M2	97.5(3)	P1-Rh-M1	163.9(3)
P1-Rh-O	76.9(2)	P1-Rh-P2	97.4(1)
Rh-P1-C9	121.9(4)	Rh-P1-C3	116.1(4)
Rh-P1-C1	106.6(4)	C3-P1-C9	100.5(5)
C1-P1-C9	105.6(5)	C1-P1-C9	104.4(5)
Rh-P2-C33	111.1(4)	Rh-P2-C27	117.9(4)
Rh-P2-C21	116.8(4)	C27-P2-C33	104.1(5)
C21-P2-C33	102.5(5)	C21-P2-C27	102.6(5)
Rh-O-C2	120.6(8)	P1-C1-C2	111.8(8)
O-C2-C1	120.1(10)	C1-C2-C15	119.9(10)
O-C2-C15	120.0(11)	C40-C39-C44	105.1(10)
C39-C40-C41	106.0(11)	C40-C41-C45	100.0(9)
C40-C41-C42	100.7(10)	C42-C41-C45	101.7(9)
C41-C42-C43	106.9(12)	C42-C43-C44	105.7(11)
C39-C44-C43	100.4(10)	C43-C44-C45	105.1(10)
C39-C44-C45	100.4(9)	C41-C45-C44	91.6(10)

^a M1 and M2 are the midpoints of the two olefinic C42-C43 and C39-C40 bonds.

Concluding Remarks

The formation of P-C coupling products is observed when the lithium enolates derived from acetone and acetophenone are reacted with Ph₂PCL and *i*-Pr₂PCL, thus extending the previously reported reaction of enolates acting as C-nucleophiles toward chlorophosphines. This provides a general synthesis of β-keto phosphine ligands. Neutral and cationic rhodium(I) complexes with two keto phosphines were inactive in the hydrogenation of hexene. Their deprotonation led to decomposition. Neutral mixed-ligand complexes with one keto phosphine provided access to cationic complexes active in catalytic hydrogenation and to enolate complexes active in the transfer hydrogenation under a hydrogen atmosphere between an alkane and an olefin. The observation that strongly electron donating ligands disfavor alkane activation in this system seems to indicate that an elementary oxidative-addition type step is not rate-determining in this process. The 14-electron species Rh{Ph₂PCH₂C(ˆO)Ph}L¹ (L¹ = phosphine) has been proposed as an important intermediate in the catalytic cycle.

Experimental Section

All operations were performed in Schlenk-type flasks under high-purity argon (Air Liquide). Solvents (Analytical Grade) were dried and distilled under argon: toluene, diethyl ether, and THF from sodium/benzophenone, pentane and heptane from sodium/potassium alloy, dichloromethane and chloroform over P₂O₅, ethanol from Mg(OEt)₂, acetone from B₂O₃,⁵² and acetonitrile from CaH₂. Nitromethane was only degassed. Elemental analyses (C, H, Cl, P) were performed by the Institut Français du Pétrole and Pascher, Regensburg, Ger-

many. IR spectra were recorded in the 4000–200 cm^{-1} region on a Perkin-Elmer 883 infrared photospectrometer. Samples were prepared as Nujol mulls, CsI or KBr pellets, or solutions using CaF_2 cells. ^1H NMR spectra were recorded at 200 MHz on an FT Bruker AC-F 200 instrument and the $^{31}\text{P}\{^1\text{H}\}$ NMR spectra at 81 MHz on an FT Bruker CXP 200 instrument. Chemical shifts (in ppm) are positive downfield relative to external SiMe_4 for ^1H and to external 85% H_3PO_4 in water for $^{31}\text{P}\{^1\text{H}\}$ NMR spectra.

The complexes $[\text{RhCl}(\text{PPh}_3)_3]$,⁵³ $[\text{RhCl}(\text{CO})(\text{PPh}_3)_2]$,⁵⁴ $[\text{Rh}(\mu\text{-Cl})(\text{NBD})_2]$,⁵⁵ $[\text{Rh}(\mu\text{-Cl})(\text{COE})_2]$,⁵⁶ $[\text{Rh}(\mu\text{-Cl})(\text{C}_2\text{H}_4)_2]$,⁵⁷ and $[\text{Ir}(\mu\text{-Cl})(\text{COE})_2]$,⁵⁸ were prepared according to published procedures. TIPF_6 was prepared under argon by reacting TIOH (from Ti_2SO_4 and BaOH) with $[\text{NH}_4]\text{PF}_6$. The phosphines PMePh_2 , $\text{P-}i\text{-Pr}_2\text{Cl}$, and PPh_2Cl were distilled before use. Triphenylphosphine was recrystallized from EtOH and stored under argon. Lithium was obtained from Metallgesellschaft. Chloroacetone was distilled before use. 1-Hexene (Aldrich) was freed from peroxides by passage through an alumina column. Cyclooctane and norbornene (solution in cyclooctane) were distilled from sodium prior to use. $\text{Ph}_2\text{PCH}_2\text{C}(\text{O})\text{Ph}$ was prepared by the method previously described and recrystallized from THF–pentane.⁶

$\text{Ph}_2\text{PCH}_2\text{C}(\text{O})\text{Me}$. Following a method similar to the synthesis of $\text{Ph}_2\text{PCH}_2\text{C}(\text{O})\text{Ph}$ but starting from acetone (90 mmol), a clear yellow liquid was obtained (bp 140 °C at 0.04 mmHg, yield 8.7 g, 40%). Anal. Found: C, 74.5; H, 6.4. Calcd for $\text{C}_{15}\text{H}_{15}\text{OP}$: C, 74.35; H, 6.24. IR (C_6H_6): 1700 $\text{s } \nu(\text{C}=\text{O}) \text{ cm}^{-1}$. ^1H NMR (CD_2Cl_2): δ 7.7–7.3 (10H, m, 2 Ph), 3.29 (2H, s, PCH_2), 2.17 (3H, s, CH_3); lit.^{10a} in C_6H_6 3.05 (2H, s, PCH_2). $^{31}\text{P}\{^1\text{H}\}$ NMR ($\text{C}_7\text{H}_8/\text{C}_6\text{D}_6$): δ –20.2.

$\text{Ph}_2\text{PCH}_2\text{C}(\text{O})\text{-}t\text{-Bu}$ was synthesized in a manner analogous to that for **L**, starting from methyl *tert*-butyl ketone (90 mmol): white solid (11.5 g, 45%). Anal. Found: C, 76.1; H, 7.5. Calcd for $\text{C}_{18}\text{H}_{21}\text{OP}$: C, 76.0; H, 7.4. IR (CH_2Cl_2): 1696 $\text{s } \nu(\text{C}=\text{O}) \text{ cm}^{-1}$. ^1H NMR (CD_2Cl_2): δ 7.5–7.3 (10H, m, Ph), 3.36 (2H, s, PCH_2), 1.10 (9H, s, $\text{C}(\text{CH}_3)_3$). $^{31}\text{P}\{^1\text{H}\}$ NMR ($\text{C}_7\text{H}_8/\text{C}_6\text{D}_6$): δ –21.6.

$i\text{-Pr}_2\text{PCH}_2\text{C}(\text{O})\text{Ph}$ was synthesized in a manner analogous to that for **L**, starting from acetophenone and $\text{P-}i\text{-Pr}_2\text{Cl}$ (89 mmol): yellow liquid (bp 105–120 °C at 0.002–0.005 mmHg), 12.6 g, 60%. Anal. Found: C, 71.2; H, 9.0. Calcd for $\text{C}_{14}\text{H}_{21}\text{OP}$: C, 71.2; H, 9.0. IR (CH_2Cl_2): 1670 $\text{s } \nu(\text{C}=\text{O}) \text{ cm}^{-1}$. ^1H NMR (CD_2Cl_2): δ 8.05–7.95 (2H, m, *meta*), 7.6–7.4 (3H, m, *ortho* and *para*), 3.12 (2H, d, $J(\text{PH})$ 1.34, PCH_2), 1.85 (2H, m, $\text{CH}(\text{CH}_3)_2$), 1.17–1.06 (12H, m, $\text{CH}(\text{CH}_3)_2$). $^{31}\text{P}\{^1\text{H}\}$ NMR ($\text{C}_7\text{H}_8/\text{C}_6\text{D}_6$): δ 5.2.

$\text{Ph}_2\text{PCH}_2\text{C}(\text{O})(\text{p-C}_6\text{H}_4\text{F})$ was synthesized as described in ref 6 for **L**, starting from (*p*-fluorophenyl)acetophenone (103 mmol): white solid; 13.2 g, 45%. Anal. Found: C, 74.1; H, 5.3. Calcd for $\text{C}_{20}\text{H}_{16}\text{FOP}$: C, 74.5; H, 5.0. IR (CH_2Cl_2): 1670 $\text{s } \nu(\text{C}=\text{O})$, 1595 s, 1506 ms, 1480 $\text{m } \nu(\text{C}=\text{O}) \text{ cm}^{-1}$. ^1H NMR (CD_2Cl_2): δ 7.5–7.3 (14H, m, aromatic), 3.79 (2H, s, PCH_2). $^{31}\text{P}\{^1\text{H}\}$ NMR (CD_2Cl_2): δ –19.2.

$[\text{Rh}(\mu\text{-Cl})\{\text{Ph}_2\text{PCH}_2\text{C}(\text{O})\text{Ph}\}(\text{C}_2\text{H}_4)_2]$ (1**).** A suspension of $[\text{Rh}(\mu\text{-Cl})(\text{C}_2\text{H}_4)_2]$ (1.27 g, 3.27 mmol) and **L** (1.99 g, 6.54 mmol) in pentane (70 mL) was stirred overnight. The solid was filtered off and washed with pentane. Recrystallization from toluene/pentane yielded an orange powder (2.77 g, 90%). Anal. Found: C, 55.7; H, 4.4; Cl, 7.2; P, 6.7. Calcd for $\text{C}_{44}\text{H}_{42}\text{-Cl}_2\text{O}_2\text{P}_2\text{Rh}_2$: C, 56.1; H, 4.5; Cl, 7.5; P, 6.6. IR (CsI): 1665 vs $\nu(\text{C}=\text{O})$, 1522 w $\nu(\text{C}=\text{C})$, 272 m and 258 m $\nu(\text{Rh}-\text{Cl})$. IR

(polychlorotrifluoroethylene): 3063 w, 1523 w $\nu(\text{C}=\text{C})$, 1667 s $\nu(\text{C}=\text{O}) \text{ cm}^{-1}$. ^1H NMR (C_7D_8 , 350 K): δ 8.3–7.0 (15H, m, Ph), 4.04 (2H, d, $^2J(\text{PH})$ 10.7 Hz, PCH_2), 3.12 (4H, s, C_2H_4). ^1H NMR (C_7D_8 , 230 K): 3.87 (2H, d, $^2J(\text{PH})$ 9.8 Hz, PCH_2), 3.30 (2H, br s, $\text{CH}_2\Rightarrow$), 2.43 (2H, br s, $\text{CH}_2\Rightarrow$). $^{31}\text{P}\{^1\text{H}\}$ NMR ($\text{C}_7\text{H}_8/\text{C}_6\text{D}_6$): δ 47.4 (d, $J(\text{RhP})$ 189.2 Hz).

$[\text{RhCl}\{\text{Ph}_2\text{PCH}_2\text{C}(\text{O})\text{Ph}\}\{\text{Ph}_2\text{PCH}_2\text{C}(\text{O})\text{Ph}\}]$ (2**).** Toluene (5 mL) was added with stirring to a mixture of **L** (0.30 g, 0.99 mmol) and $[\text{Rh}(\mu\text{-Cl})(\text{C}_2\text{H}_4)_2]$ (0.096 g, 0.24 mmol). The solution changed color immediately to yellow, and bubbles appeared. Upon addition of pentane a yellow solid precipitated, which was collected by filtration, recrystallized from toluene/ CH_2Cl_2 /pentane, and dried in vacuo (0.254 g, 70%). Anal. Found: C, 64.1; H, 4.5. Calcd for $\text{C}_{40}\text{H}_{34}\text{ClO}_2\text{P}_2\text{Rh}$: C, 64.3; H, 4.6. IR (CsI): 1674 s $\nu(\text{C}=\text{O})_{\text{uncoord}}$, 1575 m $\nu(\text{C}=\text{O})_{\text{coord}}$, 322 m $\nu(\text{Rh}-\text{Cl}) \text{ cm}^{-1}$. ^1H NMR (CD_2Cl_2): δ 8.3–7.0 (30H, m, Ph), 5.42 (2H, d, $^2J(\text{PH})$ 5.37 Hz, PCH_2), 4.86 (2H, d, $^2J(\text{PH})$ 12.2 Hz, PCH_2). $^{31}\text{P}\{^1\text{H}\}$ NMR ($\text{CH}_2\text{Cl}_2/\text{CD}_2\text{Cl}_2$): δ 42.4 (1 P, dd, $^1J(\text{RhP})$ 125 Hz, $^2J(\text{PP})$ 24 Hz, P^{O}), 35.8 (1 P, dd, $^1J(\text{RhP})$ 119.5 Hz, $^2J(\text{PP})$ 24 Hz, $\text{P}\sim\text{O}$).

***cis*- $[\text{Rh}\{\text{Ph}_2\text{PCH}_2\text{C}(\text{O})\text{Ph}\}_2][\text{PF}_6]$ (**3**).** Solid TIPF_6 (0.400 g, 1.1 mmol) was added to a stirred solution of **2** (0.33 g, 0.44 mmol) in CH_2Cl_2 (10 mL). Overnight the color changed from dark brown to red. The turbid solution was filtered over Celite and evaporated to ca. 2 mL, and layering with ether yielded red crystals (0.35 g, 94%). Anal. Found: C, 55.8; H, 4.1. Calcd for $\text{C}_{40}\text{H}_{34}\text{F}_6\text{O}_2\text{P}_3\text{Rh}$: C, 56.1; H, 4.0. IR (THF): 1565 vs $\nu(\text{C}=\text{O}) \text{ cm}^{-1}$. ^1H NMR (CD_2Cl_2): δ 8.25–7.18 (30H, m, Ph), 4.30 (4H, d, $^2J(\text{PH})$ 10.7 Hz, PCH_2). $^{31}\text{P}\{^1\text{H}\}$ NMR (THF/THF- d_6): δ 57.5 (2P, d, $^1J(\text{RhP})$ 190.8 Hz), –142.3 (1P, sept, $^1J(\text{PF})$ 705 Hz, PF_6).

$[\text{Rh}\{\text{Ph}_2\text{PCH}_2\text{C}(\text{O})\text{Ph}\}(\text{THF})_2]$ (4**).** Solid TIPF_6 (0.15 g, 0.43 mmol) was added to a red solution of **1** (0.16 g, 0.18 mmol) in THF (20 mL). After 15 h the dark red solution was filtered over Celite and analyzed only by $^{31}\text{P}\{^1\text{H}\}$ NMR and IR spectroscopic methods. Satisfactory analyses could not be obtained for stability reasons. A sample was evaporated to dryness and dissolved in C_6D_6 . IR (THF): 1520 s $\nu(\text{C}=\text{O}) + \nu(\text{C}=\text{C}) \text{ cm}^{-1}$. ^1H NMR (C_6D_6): δ 8.4–6.7 (15H, m, Ph), 5.22 (1H, d, $^2J(\text{PH})$ 3.9 Hz, PCH), 3.68 (4H, br, THF), 1.81 (4H, br, THF). $^{31}\text{P}\{^1\text{H}\}$ NMR (THF/ C_6D_6): δ 47.6 (1P, d, $^1J(\text{RhP})$ 184 Hz).

***trans*- $[\text{RhCl}\{\text{Ph}_2\text{PCH}_2\text{C}(\text{O})\text{Ph}\}(\text{CO})(\text{PPh}_3)]$ (**5**).** To solid $[\text{RhCl}(\text{CO})(\text{PPh}_3)_2]$ (0.22 g, 0.32 mmol) and **L** (0.10 g, 0.34 mmol) was added toluene (25 mL) to give a yellow solution. After it was stirred for 10 min, the solution was filtered and concentrated and pentane added to precipitate a yellow powder. It was washed with pentane and recrystallized at –20 °C from toluene/pentane to yield **5** (0.22 g, 95%). Anal. Found: C, 64.1; H, 4.6; Cl, 4.8. Calcd for $\text{C}_{39}\text{H}_{32}\text{ClO}_2\text{P}_2\text{Rh}$: C, 63.9; H, 4.4; Cl, 4.8. IR (CsI): 1974 vs $\nu(\text{C}=\text{O})$, 1672 s $\nu(\text{C}=\text{O})$, 302 m $\nu(\text{Rh}-\text{Cl})$. IR (CHCl_3): 1977 vs $\nu(\text{C}=\text{O})$, 1671 s $\nu(\text{C}=\text{O}) \text{ cm}^{-1}$. ^1H NMR (CDCl_3): δ 7.9–7.2 (30H, m, Ph), 4.49 (2H, s, PCH_2). $^{31}\text{P}\{^1\text{H}\}$ NMR ($\text{CH}_2\text{Cl}_2/\text{CD}_2\text{Cl}_2$): AB part of an ABX pattern ($\text{X} = \text{Rh}$), δ 26.6 (dd, 1 P, $^1J(\text{RhP})$ 127 Hz, $^2J(\text{PP})$ 387 Hz), 21.6 (dd, 1 P, $J(\text{RhP})$ 130 Hz, $^2J(\text{PP})$ 387 Hz).

$[\text{Rh}\{\text{Ph}_2\text{PCH}_2\text{C}(\text{O})\text{Ph}\}(\text{CO})(\text{PPh}_3)][\text{PF}_6]$ (6**).** A solution of **L** (0.177 g, 0.58 mmol) in CH_2Cl_2 (10 mL) was added with stirring to a solution of $[\text{RhCl}(\text{CO})(\text{PPh}_3)_2]$ (0.40 g, 0.58 mmol) in CH_2Cl_2 (7.5 mL) and acetone (10 mL). After 10 min, TIPF_6 (0.203 g, 0.58 mmol) was added and the solution changed color from yellow to red while a precipitate of TiCl_4 appeared overnight. Filtration, concentration, and layering with EtOH (4 mL) and ether (30 mL) yielded orange crystals (0.480 g, 98%). Anal. Found: C, 55.6; H, 3.7; P, 10.5. Calcd for $\text{C}_{39}\text{H}_{32}\text{-F}_6\text{O}_2\text{P}_3\text{Rh}$: C, 55.6; H, 3.8; P, 11.0. IR (KBr): 1995 vs $\nu(\text{C}=\text{O})$, 1555 vs $\nu(\text{C}=\text{O})$, 845 vs $\nu(\text{PF}) \text{ cm}^{-1}$. ^1H NMR (CD_2Cl_2): δ 7.35–7.9 (30H, m, Ph), 4.63 (2H, d, $^2J(\text{PH})$ 10.3 Hz, PCH_2). $^{31}\text{P}\{^1\text{H}\}$ NMR (CD_2Cl_2): AB part of an ABX pattern ($\text{X} = \text{Rh}$), δ 44.7 (1P, dd, $^1J(\text{RhP})$ 120 Hz, $^2J(\text{PP})$ 296 Hz, P^{O}),

(53) Osborn, J. A.; Jardine, F. H.; Young, J. F.; Wilkinson, G. *J. Chem. Soc. A* **1966**, 1711.

(54) Stephenson, T. A.; Wilkinson, G. *J. Inorg. Nucl. Chem.* **1966**, *28*, 945.

(55) Abel, E. W.; Bennett, M. A.; Wilkinson, G. *J. Chem. Soc.* **1959**, 3178.

(56) Hoffmann, P.; Meier, C.; Englert, U.; Schmidt, M. U. *Chem. Ber.* **1992**, *125*, 353.

(57) Cramer, R. *Inorg. Chem.* **1962**, *1*, 722.

(58) van der Ent, A.; Onderdelinden, A. L. *Inorg. Synth.* **1990**, *28*, 90.

29.9 (1P, dd, $^1J(\text{RhP})$ 132, $^2J(\text{PP})$ 296 Hz, PPh_3), -144 (sept, 1 P, $^1J(\text{PF})$ 705 Hz, PF_6).

[Rh{Ph₂PCH₂C(-O)Ph}(CO)(PPh₃)] (7). A solution of **L** (0.031 g, 0.10 mmol) in toluene (5 mL) was added to a suspension of $[\text{RhCl}(\text{CO})(\text{PPh}_3)_2]$ (0.069 g, 0.10 mmol) in toluene (5 mL). After the mixture was stirred for 10 min, NaOMe/MeOH (1.5 mL, 0.1 mmol) was added; the solution became turbid due to precipitation of NaCl. After 15 min the solution was concentrated, NaCl was filtered off (through Celite), and the product was precipitated and washed with pentane: yellow powder; 0.055 g, 80%. Anal. Found: C, 67.5; H, 4.0. Calcd for $\text{C}_{39}\text{H}_{31}\text{O}_2\text{P}_2\text{Rh}$: C, 67.3; H, 4.5. IR (KBr): 1956 vs $\nu(\text{C}=\text{O})$, 1513 s $\nu(\text{C}=\text{O}) + \nu(\text{C}=\text{C})$. IR (C_7H_8): 1960 vs $\nu(\text{C}=\text{O})$, 1514 s $\nu(\text{C}=\text{O}) + \nu(\text{C}=\text{C})$ cm^{-1} . ^1H NMR (C_6D_6 , 295 K): δ 8.1–6.9 (30H, m, Ph), 5.31 (1H, overlapping dd, $^2J(\text{PH}) = ^3J(\text{RhH}) = 2.2$ Hz, PCH). $^{31}\text{P}\{^1\text{H}\}$ NMR ($\text{THF}/\text{C}_7\text{D}_8$, 200 K): AB part of an ABX pattern (X = Rh), δ 42.0 (1P, dd, $^1J(\text{RhP})$ 127.7 Hz, $^2J(\text{PP})$ 301 Hz), 26.0 (1P, dd, $^1J(\text{RhP})$ 136.5 Hz, PPh_3). $^{31}\text{P}\{^1\text{H}\}$ NMR (295 K): δ 41.1 (1P, d, $^1J(\text{RhP})$ 131 Hz, PCH), 26.6 (s br, PPh_3).

trans-[RhCl{Ph₂PCH₂C(O)Ph}₂(CO)] (8). A mixture of $[\text{Rh}(\mu\text{-Cl})(\text{COE})_2]_2$ (0.180 g, 0.25 mmol) and **L** (0.304 g, 1 mmol) was stirred in toluene (25 mL). Under CO the red solution became green. It was filtered and concentrated, and the product was precipitated with pentane. Recrystallization from THF/Et₂O yielded yellow-green crystals (0.349 g, 90%). Anal. Found: C, 63.6; H, 4.6. Calcd for $\text{C}_{41}\text{H}_{34}\text{ClO}_3\text{P}_2\text{Rh}$: C, 63.5; H, 4.4. IR (CsI): 1980 vs $\nu(\text{C}=\text{O})$, 1666 s $\nu(\text{C}=\text{O})$, 300 m $\nu(\text{Rh-Cl})$. IR (CD_2Cl_2): 1970 vs $\nu(\text{C}=\text{O})$, 1670 s $\nu(\text{C}=\text{O})$ cm^{-1} . ^1H NMR (CD_2Cl_2): δ 7.95–7.3 (30H, m, Ph), 4.46 (4H, virtual t, $^{2+4}J(\text{PH})$ 7.3 Hz, PCH_2). $^{31}\text{P}\{^1\text{H}\}$ NMR (THF, C_6D_6): δ 21.1 (2P, d, $^1J(\text{RhP})$ 128 Hz).

[Rh{Ph₂PCH₂C(O)Ph}{Ph₂PCH₂C(O)Ph}(CO)][PF₆] (9). Solid TIPF₆ (0.075 g, 0.21 mmol) was added to a solution of **8** (0.16 g, 0.21 mmol) in CH_2Cl_2 (20 mL). After being stirred for 15 h, the turbid solution was filtered over Celite, evaporated to ca. 3 mL, and layered with ether to yield orange crystals (0.17 g, 90%). Anal. Found: C, 55.6; H, 3.7. Calcd for $\text{C}_{41}\text{H}_{34}\text{F}_6\text{O}_3\text{P}_3\text{Rh}$: C, 55.7; H, 3.9. IR (CsI): 1993 vs $\nu(\text{C}=\text{O})$, 1678 s, 1561 vs $\nu(\text{C}=\text{O})$, 840 vs $\nu(\text{PF})$. IR (CD_2Cl_2): 2005 vs $\nu(\text{C}=\text{O})$, 1675 s, 1555 vs $\nu(\text{C}=\text{O})$ cm^{-1} . ^1H NMR (CD_2Cl_2 , 295 K): δ 7.9–7.3 (30H, m, Ph), 4.48 (4H, dd, $^2J(\text{PH}) = ^3J(\text{RhH}) = 4.0$ Hz, PCH_2). $^{31}\text{P}\{^1\text{H}\}$ NMR (CD_2Cl_2 , 295 K): δ 32.5 (2P, d, $^1J(\text{RhP})$ 128 Hz), -144 (sept, 1 P, $^1J(\text{PF})$ 705 Hz, PF_6).

[Rh{Ph₂PCH₂C(-O)Ph}(CO){Ph₂PCH₂C(O)Ph}] (10). NaOMe (0.35 mL of a 0.46 M MeOH solution) was added to a stirred solution of **8** (0.125 g, 0.16 mmol) in THF (10 mL). After 15 min the solution was concentrated, filtered, and layered with pentane. Yellow crystals grew overnight (0.10 g, 86%). Anal. Found: C, 66.9; H, 4.5. Calcd for $\text{C}_{41}\text{H}_{33}\text{O}_3\text{P}_2\text{Rh}$: C, 66.7; H, 4.5. IR (CD_2Cl_2): 1960 vs $\nu(\text{C}=\text{O})$, 1668 m $\nu(\text{C}=\text{O})$, 1512 s $\nu(\text{C}=\text{O}) + \nu(\text{C}=\text{C})$ cm^{-1} . ^1H NMR (CD_2Cl_2): δ 8.1–7.25 (30H, m, Ph), 5.18 (1H, ddd, $^2J(\text{PH})$ 2.8 Hz, $^3J(\text{RhH})$ 0.4 Hz, $^4J(\text{PH})$ 1.5 Hz, PCH), 4.44 (ddd, 2H, $^2J(\text{PH})$ 9.0 Hz, $^3J(\text{RhH})$ 0.6 Hz, $^4J(\text{PH})$ 1.9 Hz, PCH_2). $^{31}\text{P}\{^1\text{H}\}$ NMR ($\text{CH}_2\text{Cl}_2/\text{CD}_2\text{Cl}_2$): AB part of an ABX pattern (X = Rh), δ 39.4 (1P, dd, $^1J(\text{RhP})$ 130 Hz, $^2J(\text{PP})$ 313 Hz, PCH), 19.5 (1P, dd, $^1J(\text{RhP})$ 140 Hz, $^2J(\text{PP})$ 313 Hz, PCH_2).

[Rh{Ph₂PCH₂C(-O)Ph}(CO){P(*o*-tolyl)₃}] (11). A red solution of $[\text{Rh}(\mu\text{-Cl})(\text{COE})_2]_2$ (0.179 g, 0.25 mmol), P(*o*-tolyl)₃ (0.152 g, 0.5 mmol), and **L** (0.152 g, 0.5 mmol) in THF (10 mL) was stirred under CO until it became green. IR showed $\nu(\text{C}=\text{O})$ at 1968 and $\nu(\text{C}=\text{O})$ at 1672 cm^{-1} , respectively. Then NaOMe (0.34 mL of a 0.46 M MeOH solution) was added. Evaporation, dissolution in a minimum of toluene, filtration, evaporation, and addition of CH_2Cl_2 and heptane yielded, on evaporation, yellow crystals. These were washed with a small amount of pentane (0.325 g, 88%). Anal. Found: C, 68.1; H, 5.2. Calcd for $\text{C}_{42}\text{H}_{37}\text{O}_2\text{P}_2\text{Rh}$: C, 68.3 H, 5.0. IR (CDCl_3): 1956 vs $\nu(\text{C}=\text{O})$, 1512 s $\nu(\text{C}=\text{O}) + \nu(\text{C}=\text{C})$ cm^{-1} . ^1H NMR (CDCl_3):

δ 8.1–7.25 (27H, m, aromatic), 5.09 (1H, dd, $^2J(\text{PH}) = ^3J(\text{RhH}) = 2$ Hz, PCH), 2.36 (9H, s, Me). $^{31}\text{P}\{^1\text{H}\}$ NMR ($\text{CH}_2\text{Cl}_2/\text{C}_6\text{D}_6$): AB part of an ABX pattern (X = Rh), δ 41.1 (1P, dd, $^1J(\text{RhP})$ 134 Hz, $^2J(\text{PP})$ 300 Hz, PCH), 23.4 (1P, dd, $^1J(\text{RhP})$ 131 Hz, $^2J(\text{PP})$ 300 Hz, P(*o*-tolyl)₃).

[Rh{Ph₂PCH₂C(-O)Ph}(CO){P(*p*-tolyl)Ph₂}] (12). This complex was prepared similarly to **11**, starting from $[\text{Rh}(\mu\text{-Cl})(\text{COE})_2]_2$ (0.359 g, 0.5 mmol), $\text{PPh}_2(p\text{-tolyl})$ (0.316 g, 1 mmol), and **L** (0.304 g, 1 mmol) in toluene (10 mL). IR showed $\nu(\text{C}=\text{O})$ at 1973 and $\nu(\text{C}=\text{O})$ at 1672 cm^{-1} , respectively. Then NaOMe (2.2 mL of a 0.46 M MeOH solution) was added. Evaporation, addition of CH_2Cl_2 and heptane, filtration, and concentration yielded on standing at -20 °C yellow crystals (0.625 g, 88%). Anal. Found: C, 67.5; H, 4.6. Calcd for $\text{C}_{40}\text{H}_{33}\text{O}_2\text{P}_2\text{Rh}$: C, 67.6 H, 4.7. IR (CD_2Cl_2): 1958 vs $\nu(\text{C}=\text{O})$, 1514 s $\nu(\text{C}=\text{O}) + \nu(\text{C}=\text{C})$ cm^{-1} . ^1H NMR (CD_2Cl_2): δ 7.84–7.17 (29H, m, aromatic), 5.19 (1H, dd, $^2J(\text{PH}) = ^3J(\text{RhH}) = 2$ Hz, PCH), 2.39 (3H, s, Me). $^{31}\text{P}\{^1\text{H}\}$ NMR ($\text{CH}_2\text{Cl}_2/\text{CD}_2\text{Cl}_2$): AB part of an ABX pattern (X = Rh), δ 41.9 (1P, dd, $^1J(\text{RhP})$ 128 Hz, $^2J(\text{PP})$ 305 Hz, PCH), 28.2 (1P, dd, $^1J(\text{RhP})$ 136 Hz, $^2J(\text{PP})$ 305 Hz, $\text{PPh}_2(p\text{-tolyl})$).

[Rh{Ph₂PCH₂C(-O)Ph}(CO){P(*p*-C₆H₄F)₃}] (13). This complex was prepared similarly to **11**, starting from $[\text{Rh}(\mu\text{-Cl})(\text{COE})_2]_2$ (0.359 g, 0.5 mmol), P(*p*-C₆H₄F)₃ (0.316 g, 1 mmol), and **L** (0.304 g, 1 mmol) in toluene (10 mL). IR showed $\nu(\text{C}=\text{O})$ at 1978 and $\nu(\text{C}=\text{O})$ at 1678 cm^{-1} , respectively. Then NaOMe (2.2 mL of a 0.46 M MeOH solution) was added. Evaporation, washing of the residue with pentane, addition of CH_2Cl_2 and heptane, filtration, and slow evaporation under a stream of argon yielded an oil, which crystallized at -20 °C: yellow crystals; 0.675 g, 90%. Anal. Found: C, 62.1; H, 4.2. Calcd for $\text{C}_{39}\text{H}_{28}\text{F}_3\text{O}_2\text{P}_2\text{Rh}$: C, 62.4; H, 3.8. IR (CD_2Cl_2): 1961 vs $\nu(\text{C}=\text{O})$, 1516 s $\nu(\text{C}=\text{O}) + \nu(\text{C}=\text{C})$ cm^{-1} . ^1H NMR (CD_2Cl_2): δ 7.84–7.11 (27H, m, aromatic), 5.21 (1H, s, PCH). $^{31}\text{P}\{^1\text{H}\}$ NMR ($\text{CH}_2\text{Cl}_2/\text{CD}_2\text{Cl}_2$): δ 42.2 (1P, dd, $^1J(\text{RhP})$ 129 Hz, $^2J(\text{PP})$ 307 Hz, PCH), 25.6 (1P, dd, $^1J(\text{RhP})$ 137 Hz, $^2J(\text{PP})$ 307 Hz, P(*p*-C₆H₄F)₃).

trans-[RhCl{Ph₂PCH₂C(O)Ph}(PPh₃)₂] (14). A solution of **L** (0.030 g, 0.10 mmol) in toluene (5 mL) was added to a suspension of $[\text{RhCl}(\text{PPh}_3)_3]$ (0.092 g, 0.1 mmol) in toluene (5 mL). Upon stirring and gentle heating a red solution was obtained and characterized spectroscopically. Complex **14** is unstable and could not be isolated pure. IR (CsI): 1672 s $\nu(\text{C}=\text{O})$, 320 m $\nu(\text{Rh-Cl})$. IR (C_7H_8): 1670 s $\nu(\text{C}=\text{O})$ cm^{-1} . ^1H NMR (C_6D_6): δ 7.9–7.2 (45H, m, Ph), 4.45 (2H, m br, PCH_2). $^{31}\text{P}\{^1\text{H}\}$ NMR ($\text{C}_7\text{H}_8/\text{C}_6\text{D}_6$): δ 46.0 (1 P, dt, $^1J(\text{RhP})$ 189.9 Hz, PCH_2 *trans* to Cl), 29.2 (2 P, dd, $^1J(\text{RhP})$ 144 Hz, $^2J(\text{PP})$ 37.8 Hz, PPh_3).

[Rh{Ph₂PCH₂C(O)Ph}(PPh₃)₂][PF₆] (15). To a solution of $[\text{RhCl}(\text{PPh}_3)_3]$ (0.688 g, 0.74 mmol) in acetone (5 mL) was added a solution of **L** (0.226 g, 0.74 mmol) in acetone/ CH_2Cl_2 (5:7 mL). After the mixture was stirred for 5 min, TIPF₆ (0.260 g, 0.74 mmol) was added and a precipitate of TiCl₄ formed overnight. The solution was decanted, filtered over Celite, and evaporated to a small volume. Addition of EtOH and ether yielded red crystals. These were recrystallized from $\text{CH}_2\text{Cl}_2/\text{EtOH}/\text{ether}$: 0.717 g, 90. Anal. Found: C, 62.3; H, 4.2; P, 11.6. Calcd for $\text{C}_{56}\text{H}_{47}\text{F}_6\text{OP}_4\text{Rh}$: C, 62.5; H, 4.4; P, 11.5. IR (KBr): 1570 s $\nu(\text{C}=\text{O})$, 850 vs $\nu(\text{PF})$. IR (CH_2Cl_2): 1565 s $\nu(\text{C}=\text{O})$ cm^{-1} . ^1H NMR (CD_2Cl_2): δ 7.7–6.9 (45H, m, Ph), 4.12 (2H, d, $^2J(\text{PH})$ 9.28 Hz, PCH_2). $^{31}\text{P}\{^1\text{H}\}$ NMR ($\text{CH}_2\text{Cl}_2/\text{CD}_2\text{Cl}_2$): δ 51.2 (1P, dt, $^1J(\text{RhP})$ 188.2 Hz, $^2J(\text{PP})$ 35.6 Hz, PPh_3 *cis* to PCH_2), 47.3 (1P, ddd, $^1J(\text{RhP})$ 147.5 Hz, $^2J(\text{PP})$ 35.6, 300.1 Hz, PCH_2), 28.8 (1P, ddd, $^1J(\text{RhP})$ 142.4 Hz, $^2J(\text{PP})$ 35.6, 300.1 Hz, PPh_3 *trans* to PCH_2), -144 (1 P, sept, $^1J(\text{PF})$ 705 Hz, PF_6).

[Rh{Ph₂PCH₂C(-O)Ph}(PPh₃)₂] (16). A solution of **L** (0.226 g, 0.74 mmol) in toluene (5 mL) was added to a solution of $[\text{RhCl}(\text{PPh}_3)_3]$ (0.688 g, 0.74 mmol) in toluene (5 mL). After 10 min of stirring NaOMe/MeOH (1.5 mL, 0.74 mmol) was

added; the solution became turbid due to precipitation of NaCl. After 15 min the solution was concentrated and NaCl was filtered off (through Celite). The product was precipitated and washed with pentane. Recrystallization from CH₂Cl₂/pentane yielded orange crystals (0.65 g, 90%). Anal. Found: C, 69.5; H, 4.9; P, 9.4. Calcd for C₅₆H₄₆OP₃Rh·0.5CH₂Cl₂: C, 69.7; H, 4.9; P, 9.55. IR (KBr): 1523 s ν(C=O) + ν(C=C). IR (C₇H₈): 1515 s ν(C=O) + ν(C=C) cm⁻¹. ¹H NMR (C₆D₆): δ 7.8–6.7 (45H, m, Ph), 5.20 (1H, d, ²J(PH) 3.2 Hz, PCH). ³¹P{¹H} NMR (CH₂Cl₂/C₆D₆): values from spectral simulation (PANIC Bruker), δ 49.8 (1P, dt, ¹J(RhP) 174, ²J(PP) 38 Hz, PPh₃ *cis* to PCH), 39.2 (1P, ddd, ¹J(RhP) 149 Hz, ²J(PP) 304, 38 Hz, PCH), 30.3 (1P, ddd, ²J(PP) 304, 38 Hz, ¹J(RhP) 147 Hz, PPh₃ *trans* to PCH).

[Rh{Ph₂PCHC(O)(*p*-C₆H₄F)}(PPh₃)₂] (17). As for **16** starting from Ph₂PCH₂C(O)(*p*-C₆H₄F) (0.13 g, 0.40 mmol), [RhCl(PPh₃)₃] (0.37 g, 0.40 mmol), and NaOMe (0.8 mL of a 0.5 M MeOH solution). Recrystallization from CH₂Cl₂/pentane yielded orange crystals, which were washed with a small amount of cold pentane (0.18 g, 48%). Anal. Found: C, 70.7; H, 4.9. Calcd for C₅₆H₄₅FOP₃Rh: C, 70.9; H, 4.8. IR (CD₂Cl₂): 1525 s ν(C=O) + ν(C=C) cm⁻¹. ¹H NMR (CD₂Cl₂): δ 7.8–6.7 (44H, m, Ph), 4.75 (1H, s, PCH). ³¹P{¹H} NMR (CH₂Cl₂/C₆D₆): δ 50.9 (1P, dt, ¹J(RhP) 174 Hz, ²J(PP) 37 Hz, PPh₃ *trans* to O), 40.3 (1P, ddd, ¹J(RhP) 149 Hz, ²J(PP) 303, 37 Hz, PCH), 30.8 (1P, ddd, ¹J(RhP) 149 Hz, ²J(PP) 303, 37 Hz, PPh₃ *trans* to PCH).

[RhCl{Ph₂PCH=C(Ph)OPPh₂}(PPh₃)₃] (18). A solution of commercial PPh₂Cl (25.3 μL, 0.14 mmol) and pyridine (one drop) in THF (5 mL) was added to a stirred solution of **16** (0.122 g, 0.13 mmol) in THF (10 mL). After 1 h, the solution was filtered and the solvent removed *in vacuo*. The yellow precipitate was washed with pentane and recrystallized from CH₂Cl₂/pentane (0.087 g, 75%). Anal. Found: C, 67.8; H, 4.4; Cl, 4.6. Calcd for C₅₀H₄₁ClOP₃Rh: C, 67.5; H, 4.65; Cl, 4.0. IR (C₆D₆): 1593 m, 1569 m, 1517 w cm⁻¹. ¹H NMR (C₆D₆): δ 7.8–6.8 (40H, m, Ph), 5.92 (1H, br, PCH). ³¹P{¹H} NMR (THF/C₆D₆): δ 151.0 (1P, ddd, ¹J(RhP) 203 Hz, ²J(PP) 61, 30 Hz, Ph₂PO), 30.0 (1P, ddd, ¹J(RhP) 137 Hz, ²J(PP) 341, 30 Hz, PPh₃ *trans* to PCH), 2.6 (1P, ddd, ¹J(RhP) 132 Hz, ²J(PP) 341, 61 Hz, PCH).

[Rh{Ph₂PC[C(O)Ph]=C(O)NHPPh}(PPh₃)₂] (19). Phenylisocyanate (0.44 mL, ca. 4 mmol) was added dropwise to a stirred solution of **16** (0.186 g, 0.2 mmol) in THF (10 mL). After 3 days, the solution was filtered and concentrated and pentane was added. The precipitate was washed with pentane and recrystallized from CH₂Cl₂/pentane: 0.10 g, 50%. Anal. Found: C, 71.7; H, 4.9; N, 1.6. Calcd for C₆₃H₅₁NO₂P₃Rh: C, 72.1; H, 4.9; N, 1.3. IR (KBr): 1620 m, 1585 s, 1560 m, 1485 w cm⁻¹. ¹H NMR (CH₂Cl₂): δ 10.37 (br, 1H, NH, exchanges with D₂O), 8.0–7.0 (50H, m, Ph). ³¹P{¹H} NMR (THF/C₆D₆): δ 51.4 (1P, ddd, ¹J(RhP) 148 Hz, ²J(PP) 296, 36 Hz, PC), 49.9 (1P, dt, ¹J(RhP) 216 Hz, ²J(PP) 36 Hz, PPh₃ *trans* to O), 29.7 (ddd, 1P, ¹J(RhP) 141 Hz, ²J(PP) 296, 36 Hz, PPh₃ *trans* to P).

[Rh{Ph₂PCH₂C(O)Ph}(PPh₃)₂][PF₆] (20). To a solution of [Rh(μ-Cl)(NBD)]₂ (1.08 g, 1.16 mmol) in CH₂Cl₂ was added PPh₃ (0.305 g, 1.16 mmol), **L** (0.353 g, 1.16 mmol), and TlPF₆ (0.407 g, 1.16 mmol). When the mixture was stirred overnight, a precipitate of TlCl formed, which was filtered off (Celite). Evaporation to a small volume and layering with EtOH and ether yielded orange crystals (0.53 g, 85%). Anal. Found: C, 59.4; H, 4.5; P, 9.9. Calcd for C₄₅H₄₀F₆OP₃Rh: C, 59.6; H, 4.4; P, 10.3. IR (KBr): 1670 w, 1620 s ν(C=O), 846 vs ν(PF) cm⁻¹. ¹H NMR (CD₂Cl₂): δ 8.0–7.2 (30H, m, Ph), 4.06 (4H, dd, ²J(RhH) 4.4 Hz, ³J(HH) 1.9 Hz, CH), 3.92 (2H, large d, ³J(HH) 1.9 Hz, CH), 3.03 (2H, d, ²J(PH) 9.8 Hz, PCH₂), 1.47 (br s, 2H, CH₂). ³¹P{¹H} NMR (CD₂Cl₂): AB part of an ABX pattern (X = Rh), δ 29.0 (1P, dd, ¹J(RhP) 150 Hz, ²J(PP)

33 Hz, PCH₂), 23.1 (1P, dd, ¹J(RhP) 142 Hz, ²J(PP) 33 Hz, PPh₃), -144 (1P, sept, ¹J(PF) 705 Hz, PF₆).

[Rh{Ph₂PCH₂C(=O)Ph}(NBD)] (21). To a stirred suspension of [Rh(μ-Cl)(COE)₂]₂ (0.232 g, 0.32 mmol) in toluene (10 mL) was added norbornadiene (0.8 mL) and **L** (0.197 g, 0.64 mmol). After 10 min, IR spectroscopy showed bands at 1672 s (ν(C=O) of P~O), 1645 m, and 1545 s cm⁻¹. On addition of NaOMe/MeOH (1.3 mL of a 0.5 M MeOH solution) the yellow solution became orange and cloudy due to precipitation of NaCl. After being stirred for 15 min, the solution was concentrated, filtered, and taken to dryness. Recrystallization of the residue from CH₂Cl₂/heptane yielded 0.214 g (66%) of air-sensitive orange crystals. Anal. Found: C, 64.8; H, 4.95. Calcd for C₂₇H₂₄OPRh: C, 65.1; H, 4.85. IR(CH₂Cl₂): 1510 s ν(C=O) + ν(C=C) cm⁻¹. ¹H NMR (CD₂Cl₂): δ 7.78–7.28 (15H, m, Ph), 5.45 (2H, br, =CH-, NBD), 4.88 (1H, s, PCH), 3.97 (2H, br, CH, NBD), 3.74 (2H, br, =CH, NBD), 1.51 (2H, m, CH₂, NBD). ³¹P{¹H} NMR (CH₂Cl₂/CD₂Cl₂): δ 25.0 (d, ¹J(RhP) 178 Hz).

[Rh{Ph₂PCH₂C(=O)Ph}(COD)] (22). This complex was prepared similarly to **21** using 0.8 mL of cyclooctadiene. Recrystallization from CH₂Cl₂/heptane yielded 0.28 g (85%) of a slightly air-sensitive orange powder. Anal. Found: C, 65.5; H, 5.4. Calcd for C₂₈H₂₈OPRh: C, 65.4; H, 5.5. IR (CH₂Cl₂): 1515 s ν(C=O) + ν(C=C) cm⁻¹. ¹H NMR (C₆D₆): δ 8.13–6.9 (15H, m, Ph), 5.62 (br, 2H, COD), 5.0 (s, 1H, PCH), 3.71 (br, 2H, =CH), 2.12 (m, 4H, CH₂), 1.76 (m, 4H, CH₂). ³¹P{¹H} NMR (CH₂Cl₂/CD₂Cl₂): δ 24.9 (d, ¹J(RhP) 155 Hz).

[Rh{Ph₂PCH₂C(=O)Me}(NBD)] (23). This complex was prepared similarly to **21** by starting from [Rh(μ-Cl)(COE)₂]₂ (0.334 g, 0.465 mmol) in toluene (15 mL), norbornadiene (1.5 mL), Ph₂PCH₂C(O)Me (0.237 g, 0.97 mmol), and NaOMe/MeOH (2.0 mL). Slow evaporation of a CH₂Cl₂/heptane (5:30 mL) solution yielded an air-sensitive orange powder (0.32 g, 79%). Anal. Found: C, 60.7; H, 4.9. Calcd for C₂₂H₂₂OPRh: C, 60.6; H, 5.1. IR (CH₂Cl₂): 1520 s ν(C=O) + ν(C=C) cm⁻¹. ¹H NMR (CDCl₃): δ 7.78–7.28 (10H, m, Ph), 5.39 (2H, br, =CH-, NBD), 4.16 (1H, dd, ²J(PH) 2 Hz, ³J(RhH) 0.7 Hz, PCH), 3.90 (2H, br, CH, NBD), 3.63 (2H, br, =CH, NBD), 2.01 (3H, s, C(O)Me), 1.44 (2H, m, CH₂, NBD). ³¹P{¹H} NMR (CH₂Cl₂/C₆D₆): δ 24.9 (d, ¹J(RhP) 177 Hz).

[Rh{Ph₂PCH₂C(=O)(*p*-C₆H₄F)}(NBD)] (24). This complex was prepared similarly to **21** by starting from [Rh(μ-Cl)(COE)₂]₂ (0.35 g, 0.48 mmol) in norbornadiene (4 mL), Ph₂PCH₂C(O)(*p*-C₆H₄F) (0.338 g, 0.98 mmol) in toluene (10 mL), and NaOMe/MeOH (2.0 mL, 0.5 M). After total evaporation, a CH₂Cl₂/heptane solution (10 mL/20 mL) was added in two portions and the solution was filtered through Celite. On concentration orange crystals formed, which were filtered off and washed twice with pentane (3 mL each): yield 0.235 g, 48%. Anal. Found: C, 62.5; H, 4.3. Calcd for C₂₇H₂₃FOPRh: C, 62.8; H, 4.5. IR (CH₂Cl₂): 1520 s ν(C=O) + ν(C=C) cm⁻¹. ¹H NMR (CD₂Cl₂): δ 7.8–7.0 (14H, m, Ph), 5.43 (2H, br, =CH, NBD), 4.84 (1H, s, PCH), 3.97 (2H, br, CH, NBD), 3.73 (2H, br, =CH, NBD), 1.50 (2H, m, CH₂, NBD). ³¹P{¹H} NMR (CH₂Cl₂/C₆D₆): δ 25.1 (d, ¹J(RhP) 178 Hz).

[Rh{ⁱPr₂PCH₂C(=O)Ph}(NBD)] (25). This complex was prepared similarly to **21** by starting from [Rh(μ-Cl)(COE)₂]₂ (0.734 g, 1.02 mmol) in toluene (20 mL), norbornadiene (2.4 mL), *i*-Pr₂PCH₂C(O)Ph (0.483 g, 2.04 mmol) in toluene (10 mL), and NaOMe/MeOH (4.0 mL, 0.5 M). After filtration, CH₂Cl₂ (5 mL) and heptane (30 mL) were added and some rhodium metal filtered off. The solution was evaporated to give a dark red oil, which crystallized at -20 °C. Recrystallization from pentane at -20 °C gave red-orange crystals (0.60 g, 68%). Anal. Found: C, 58.8; H, 6.7. Calcd for C₂₁H₂₈OPRh: C, 58.6; H, 6.6. IR (CHCl₃): 1521 s ν(C=O) + ν(C=C) cm⁻¹. ¹H NMR (CDCl₃): δ 8.05–7.95 (m, 2H, *meta*),

7.20–7.35 (3H, m, *ortho* and *para*), 5.39 (2H, br, =CH–, NBD), 4.38 (1H, t, $^2J(\text{PH}) \approx ^3J(\text{RhH}) = 1 \text{ Hz}$, PCHCO), 3.96 (2H, br, =CH–, NBD), 3.87 (2H, br), 1.95 (2H, m, CH₂, NBD), 1.5 (2H, m, P(CHMe₂)₂), 1.30–1.15 (12H, m, P(CHMe₂)₂). $^{31}\text{P}\{^1\text{H}\}$ NMR (CH₂Cl₂/C₆D₆): δ 47.7 (d, $^1J(\text{RhP})$ 167 Hz).

[Ir{Ph₂PCH=C(O)Ph}(COD)] (26). This complex was prepared similarly to **21** by starting from [Ir(μ -Cl)(COE)₂]₂ (0.249 g, 0.28 mmol) in toluene (10 mL), cyclooctadiene (0.8 mL), and **L** (0.169 g, 0.56 mmol) to give an orange solution. After 10 min NaOMe/MeOH (1.1 mL) was added and the solution became red. After 10 min the solvent was evaporated, CH₂Cl₂ and heptane were added, and the orange solution was filtered. Slow evaporation and cooling to –20 °C yielded air-sensitive orange crystals (0.287 g, 85%). Anal. Found: C, 55.6; H, 4.6. Calcd for C₂₈H₂₈OPIr: C, 55.7; H, 4.7. IR (CH₂-Cl₂): 1518 s $\nu(\text{C}=\text{O}) + \nu(\text{C}=\text{C}) \text{ cm}^{-1}$. ^1H NMR (CD₂Cl₂): δ 7.88–7.3 (15H, m, Ph), 5.10 (1H, d, $^2J(\text{PH})$ 2.9 Hz, PCH), 5.08 (2H, br, CH, COD), 3.39 (2H, br, CH, COD), 2.24 (4H, m, CH₂, COD), 1.88 (4H, m, CH₂, COD). $^{31}\text{P}\{^1\text{H}\}$ NMR (C₇H₈/C₆D₆): δ 20.3 (s).

[Ir{Ph₂PCH=C(O)Ph}H₂(COD)] (27). An orange solution of **26** in CD₂Cl₂ became colorless by bubbling hydrogen through it, but a pure solid could not be isolated. ^1H NMR (CD₂Cl₂): δ 7.88–7.3 (15H, m, Ph), 5.54 (1H, br, =CH, COD), 5.12 (1H, d, $J(\text{PH})$ 4.3 Hz, PCH), 5.02 (1H, br, =CH, COD), 3.80 (1H, br, =CH, COD), 3.58 (1H, br, COD), 2.68 (2H, m, CH₂), 2.4 (2H, m, CH₂), 2.08 (4H, m, CH₂), –11.03 (1H, d, $J(\text{PH})$ 18 Hz, IrH *trans* to olefinic double bond), –18.04 (1H, d, $J(\text{PH}) = 12 \text{ Hz}$, IrH *trans* to oxygen). $^{31}\text{P}\{^1\text{H}\}$ NMR (C₆D₆/C₇H₈): δ 27.6 (s).

Catalysis. Hydrogenation Reactions. The catalytic reactions were carried out at atmospheric pressure in a thermostated double-jacketed glass reactor (50 mL). The catalyst precursor was weighed in. Two vacuum/hydrogen cycles were applied, and the solvent and 1-hexene were added by syringe. The solution was stirred with a magnetic stirring bar, and the clock was started at the same time. The reaction could be followed by pressure decrease of the hydrogen reservoir. Samples were taken by a syringe through a septum and analyzed by GC on a Sil5 or PONA column.

Transfer-Dehydrogenation Reactions. Reactions conducted at atmospheric pressure were similar to hydrogenations, using cyclooctane as solvent and an olefin as hydrogen acceptor. Reactions performed at 0.6–7 MPa pressure were run in a thermostated double-jacketed stainless-steel autoclave (100 mL) containing a magnetic stirring bar. In a typical run, a given quantity of the catalyst precursor was weighed in a Schlenk flask. Under argon, cyclooctane and a norbornene/cyclooctane solution were added by syringe with stirring. After a few minutes of stirring a yellow homogeneous solution resulted which was transferred via cannula into the thermostated autoclave. After two hydrogen purges (0.5 MPa) to free the autoclave from argon, it was pressurized with hydrogen. Consumption of hydrogen was followed by pressure decrease of the ballast but was not determined with high precision, product analysis by GC being much more precise and reliable. Before complete consumption of the hydrogen acceptor, the autoclave was cooled with dry ice. A sample of the solution was analyzed by GC on a Sil5 column. Sometimes the remaining solution was transferred to a Schlenk flask and evaporated to dryness, the residue dissolved in CD₂Cl₂, and this solution analyzed by ^1H NMR and IR spectroscopy.

X-ray Crystallographic Analysis of 3·H₂O. Details are given in Table 8. Suitable single crystals of 3·H₂O were obtained by slow diffusion of ether in a CH₂Cl₂ solution at room temperature. Adventitious water gave rise to crystallization of the complex as a solvate. A single crystal was cut out from a cluster of crystals and mounted on a rotation-free goniometer

head. A systematic search in reciprocal space using an Enraf-Nonius CAD4-F automatic diffractometer showed that crystals of 3·H₂O belong to the triclinic system. Quantitative data were obtained at room temperature. The resulting data set was transferred to a VAX computer, and for all subsequent calculations the Enraf-Nonius Molen package was used.⁵⁹ Three standard reflections measured every 1 h during the entire data collection period showed no significant trend. The raw data were converted to intensities and corrected for Lorentz and polarization factors. Absorption corrections derived from the Φ scans of four reflections were applied. The structure was solved using the heavy-atom method. After refinement of the heavy atoms, a difference-Fourier map revealed maximas of residual electronic density close to the positions expected for hydrogen atoms; they were introduced in structure factor calculations by their computed coordinates (C–H = 0.95 Å) and isotropic temperature factors such as $B(\text{H}) = 1.3B_{\text{eqv}}(\text{C}) \text{ \AA}^2$ but not refined. Full least-squares refinements were carried out: $\sigma^2(F^2) = \sigma^2_{\text{counts}} + (pI)^2$. A final difference map revealed no significant maxima. The scattering factor coefficients and anomalous dispersion coefficients come from ref 60.

X-ray Crystallographic Analysis of 6 and 20. Details are given in Table 8. No correction for absorption was applied for **6** and **20** in view of the low absorption coefficient. Only the observed reflections were used in the structure solution and refinement. The structures were solved by Patterson and Fourier methods. The refinements were carried out by full-matrix least squares with isotropic and then with anisotropic thermal parameters in the last cycles for all non-hydrogen atoms. Hydrogen atoms were placed at their geometrically calculated positions (C–H = 0.96 Å) and refined "riding" on the corresponding carbon atoms. The weighting scheme used in the final cycles of refinement was $w = [\sigma^2(F_o) + gF_o^2]^{-1}$; at convergence the K and g values were 0.743 and 0.0068 for **6** and 0.595 and 0.0097 for **20**. The atomic scattering factors, corrected for the real and imaginary parts of anomalous dispersion, were taken from ref 60. All calculations were carried out on the Gould Povernode 6040 of the "Centro di Studio per la Strutturistica Diffattometrica" del CNR, Parma, Italy, using SHELX-76 and SHELXS-86 programs.⁶¹

The final atomic coordinates for the non-hydrogen atoms are given in Tables S-I–S-III, respectively. Additional material available from the Cambridge Crystallographic Data Centre comprises H-atom coordinates, thermal parameters, and complete listings of bond distances and angles.

Acknowledgment. We are grateful to the Centre National de la Recherche Scientifique (CNRS) and the Institut Français du Pétrole (IFP) for financial support. J.N. is grateful to Dr. L. Saussine, Dr. D. Commereuc, and Dr. G. Serpe (all IFP) for fruitful discussions.

Supporting Information Available: Positional parameters for the non-hydrogen atoms (Tables S-I–S-III), positional parameters for the hydrogen atoms (Tables S-IV–S-VI), temperature factors for anisotropic atoms (Tables S-VII–S-X), and all bond distances and angles (Tables S-X–S-XII) for complexes 3·H₂O, **6**, and **20**, respectively (30 pages). Ordering information is given on any current masthead page.

OM960814H

(59) Molen, An Interactive Structure Determination Procedure; Enraf-Nonius, Delft, The Netherlands, 1990.

(60) Cromer, D. T.; Waber, J. T. *International Tables for X-ray Crystallography*; Kynoch Press: Birmingham, England, 1974; Vol. IV.

(61) Sheldrick, G. M. SHELX-76, Program for Crystal Structure Determination; University of Cambridge, Cambridge, England, 1976. SHELX-86, Program for the Solution of Crystal Structures; University of Göttingen, Göttingen, Germany, 1986.